



**Ana Isabel Bastos
Valente**

Extração e purificação de RuBisCO: da biomassa residual à proteína de valor acrescentado

RuBisCOs' extraction and purification: from residual biomass to value added protein



**Ana Isabel Bastos
Valente**

Extração e purificação de RuBisCO: da biomassa residual à proteína de valor acrescentado

RuBisCOs' extraction and purification: from residual biomass to value added protein

Tese apresentada à Universidade de Aveiro para cumprimento dos requisitos necessários à obtenção do grau de Mestre em Biotecnologia Industrial e Ambiental, realizada sob as orientações científicas da Doutora Ana Paula Mora Tavares, Investigadora Auxiliar do Departamento de Química da Universidade de Aveiro e da Doutora Ana Mafalda Rodrigues Almeida Rocha, Investigadora do Departamento de Química da Universidade de Aveiro

This master thesis was developed within the AÇÃO INTEGRADA – PORTUGAL/FRANÇA PROG. PESSOA PHC PESSOA 2018/2019 Nº 441.00.

“Matar o sonho é matarmo-nos. É mutilar a nossa alma. O sonho é o que temos de realmente nosso, de impenetravelmente e inexpugnavelmente nosso.”

-Fernando Pessoa-

o júri

Presidente

Prof. Doutor Jorge Manuel Alexandre Saraiva
professor associado do Departamento de Química da Universidade de Aveiro

Doutora Ana Paula Mora Tavares
Investigadora Auxiliar do Departamento de Química da Universidade de Aveiro

Prof. Doutor Oscar Rodriguez
professor contratado do Departamento de Engenharia Química da Universidade de Santiago de Compostela

Agradecimentos

Antes de mais quero agradecer às minhas orientadoras, Doutoradas Ana Paula Tavares e Mafalda Almeida pelas orientações, acompanhamento e incentivo durante este ano.

Um agradecimento especial à Ana Maria que me orientou e acompanhou também este ano, mas que tem estado presente, em conjunto com a Dr. Ana Paula, desde o meu primeiro dia no Path e que mais do que uma orientadora vejo-a também como uma amiga/presente que Aveiro me deu. À Marguerita, à Ana Rufino e à Leonor que aturaram algumas das minhas crises existenciais (ahahah) muito obrigada pela paciência e pela capacidade que têm para transmitir calma e alegria. À Rita Teles, ao João Nunes, à Catarina Almeida, ao Bobi, ao Emanuel Capela e ao Alexandre Santiago pela alegria, música, gargalhadas e espírito que consegue sempre transformar o dia. Aos meus colegas de mestrado Ana Miguel, Daniel Castro, Guilherme Sousa e Rui Bento por me mostrarem que eu não estava sozinha e me darem alento.

Por último um agradecimento a 3 famílias. À família Path, pois é impossível eu ter nomeado todos aqueles que me tenham de alguma forma ajudado, mesmo que não tenham dado conta. Aos meus amigos que ouviram os meus desabafos e que me ajudaram a levantar. E à minha família que tornou tudo isto possível e me apoia em todos os instantes.

Obrigada a todos!!

palavras-chave

Ribulose-1,5-biphosphate carboxylase/oxygenase, extração sólido-líquido, sistemas aquosos bifásicos, líquidos iônicos, extração, purificação

Resumo

Com o crescimento da população mundial são necessárias novas fontes de proteínas. A biomassa vegetal é uma fonte promissora, pois permite a utilização de resíduos de culturas agrícolas com a capacidade de ser uma fonte contínua de biomassa sem prejudicar os ecossistemas já existentes, e a extração de proteínas de biomassa ainda fresca. Atualmente, com os métodos utilizados, é obtido um produto final que não pode ser aplicado na indústria alimentar além de que, os métodos até hoje desenvolvidos não são seletivos nem permitem atingir simultaneamente purezas e eficiências de extração próximas de 100 %. A RuBisCO (Ribulose-1,5-bifosfato carboxilase/oxigenase) é a proteína (enzima) mais abundante no planeta e pode ser aplicada nas mais diversas áreas, desde a farmacêutica à alimentar e de rações. Deste modo, nesta tese de mestrado foi desenvolvido um novo método de extração da RuBisCO e posterior separação e purificação. Para tal, foram usadas soluções aquosas de líquidos iônicos (LIs) biocompatíveis (análogos da glicina-betaína e derivados de colínio) na extração sólido-líquido da RuBisCO da folha do espinafre. Através da metodologia de superfície de resposta, foram otimizadas as condições da extração (pH, razão sólido-líquido e a concentração de LI). Nas condições ótimas, foi obtida uma extração máxima de 2.00 mg /mL de RuBisCO e um rendimento de 10.93 mg de RuBisCO /g de biomassa para o acetato de colínio ([Ch][Acetato]) e 1.86 mg /mL e um rendimento de 10.12 mg de RuBisCO /g de biomassa para o cloreto de colínio ([Ch]Cl). Os pontos ótimos determinados foram: razão sólido-líquido de 0.184, concentração de LI de 2.68 M e um pH de 9.09 para o [Ch]Cl e 11.2 para o [Ch][Acetato].

Após a extração, a separação e a purificação da RuBisCO foi realizada através da aplicação de sistema aquoso bifásicos (SABs). Os extratos provenientes da extração sólido-líquido com [Ch]Cl e [Ch][Acetato] que contêm LI e RuBisCO foram misturados individualmente com polipropileno glicol 400 g.mol⁻¹ (PPG 400) ou polietileno glicol 1000 g.mol⁻¹ (PEG 1000) e fosfato dipotássico (K₂HPO₄) formando-se dois tipos de SABs compostos por LI e polímero ou sal. Após este processo foi possível obter uma eficiência de extração da RuBisCO de 100% para a fase de LI no sistema composto por PPG400+ [Ch][Acetato] e por K₂HPO₄ + LI ([Ch][Acetato] e [Ch]Cl), no entanto, não foi possível separar a RuBisCO das restantes proteínas, tendo demonstrado estes SABs (LI+polímero e LI+sal) não serem seletivos para a purificação da RuBisCO.

Keywords

Ribulose-1,5-biphosphate carboxylase/oxygenase, solid-liquid extraction, aqueous biphasic systems, ionic liquids, extraction, purification

Abstract

With the growth of the world population, new sources of proteins are needed. Vegetable biomass is a promising source, as it allows the use of agricultural crop residues with the ability to be a continuous source of biomass without harming existing ecosystems, and the extraction of biomass proteins while still fresh. Currently, with the methods used, a final product is obtained that cannot be applied in the food industry. Furthermore, the methods developed until today are not selective and do not allow simultaneously reaching purities and extraction efficiencies close to 100%.

RuBisCO (Ribulose-1,5-bisphosphate carboxylase/oxygenase) is the most abundant protein (enzyme) on the planet and can be applied in the most diverse areas, from pharmaceuticals to food and feed. Thus, in this master's thesis, a new method of extracting RuBisCO and subsequent separation and purification was developed. For this purpose, aqueous solutions of biocompatible ionic liquids (ILs) (glycine-betaine analogues and cholinium derivatives) were used in the solid-liquid extraction of RuBisCO from the spinach leaf. Through the response surface methodology, the extraction conditions (pH, solid-liquid ratio, and IL concentration) were optimized. Under optimum conditions, a maximum extraction of 2.00 mg/ mL of RuBisCO and a yield of 10.93 mg of RuBisCO/ g of biomass for cholinium acetate ([Ch][Acetate]) and 1.86 mg/ mL and a yield of 10.12 mg RuBisCO / g biomass for cholinium chloride ([Ch]Cl). The optimum points determined were: solid-liquid ratio of 0.184, IL concentration of 2,68 M and a pH of 9.09 for [Ch]Cl and 11.2 for [Ch][Acetate].

After extraction, the separation and purification of RuBisCO were performed through the application of aqueous biphasic systems (ABSs). The extracts from the solid-liquid extraction with [Ch]Cl and [Ch][Acetate] containing IL and RuBisCO were individually mixed with polypropylene glycol 400 g.mol⁻¹ (PPG 400) or polyethylene glycol 1000 g.mol⁻¹ (PEG 1000) and dipotassium phosphate (K₂HPO₄) forming two types of ABSs composed of IL and polymer or salt. After this process, it was possible to obtain a RuBisCO extraction efficiency of 100% for the IL phase in the system composed of PPG400 + [Ch][Acetate] and K₂HPO₄ + IL ([Ch][Acetate] and [Ch]Cl), however, it was not possible to separate RuBisCO from the remaining proteins, having demonstrated that these ABSs (IL + polymer and IL + salt) are not selective for the purification of RuBisCO.

Index

1. Introduction.....	1
1.1. Scopes and objectives.....	3
1.2. RuBisCO	4
1.2.1. Structure, characterization, and mechanisms of action	4
1.2.2. RuBisCO's applications	7
1.3. RuBisCO extraction and purification methods.....	8
1.3.1. Traditional methods.....	8
1.3.2. Solid-liquid extraction.....	10
1.3.2.1. General concepts.....	10
1.3.3.2. Solid-liquid extraction using Ionic Liquids	12
1.3.3. Aqueous Biphasic Systems (ABS).....	13
1.3.3.1. General concepts.....	13
1.3.3.2. Ionic liquid-based ABS (IL-based ABS).....	16
1.4. Main goal of the thesis	17
2. Experimental Section.....	19
2.1. Materials	21
2.2. RuBisCOs' solid-liquid extraction.....	23
2.3. Response surface methodology (RSM).....	23
2.4. SDS-PAGE analysis	25
2.5. SE-HPLC analysis.....	25
2.6. RuBisCOs' purification using ABS	26
3. Results and Discussion.....	29
3.1. RuBisCOs' solid-liquid extraction.....	31
3.1.1. Effect of aqueous solutions of ILs on the RuBisCO's extraction	31
3.1.2. Effect of ILs concentration on the RuBisCO's extraction.....	33
3.1.3. Effect of cholinium-based ILs and their concentration on the RuBisCO's extraction.....	36

3.2. Response surface methodology (RSM)	39
3.2.1. Analysis of results for [Ch][Acetate]	39
3.2.2. Analysis of results for [Ch]Cl.....	41
3.3. RuBisCOs' purification with ABS	45
4. Final Remarks	51
Conclusions	53
Future work	54
5. References	55
Appendix A	63
A 1. Calibration curve for the quantification of the total amount of proteins	65
A 2. Calibration curve for the quantification of the amount of RuBisCO	65
Appendix B	67
B 1. Factorial planning for both ILs	69
B 2. Experimental data and response surface predicted values of the factorial planning for [Ch][Acetate]	70
B 3. Experimental data and response surface predicted values of the factorial planning for [Ch]Cl	72
B 4. Regression coefficients of the predicted second-order polynomial model from RSM using [Ch][Acetate]	74
B 5. Regression coefficients of the predicted second-order polynomial model from RSM using [Ch]Cl	76
B 6. Pareto charts for the standardized main effects in the factorial planning with [Ch][Acetate]	78
B 7. Pareto charts for the standardized main effects in the factorial planning with [Ch]Cl	79
B 8. ANOVA data for the extraction with [Ch][Acetate]	80
B 9. ANOVA data for the extraction with [Ch]Cl	81

B 10. Profiles for predicted values and desirability in the factorial planning with [Ch][Acetate]	82
B 11. Profiles for predicted values and desirability in the factorial planning with [Ch]Cl.....	83
Appendix C.....	85
C 1. Experimental binodal data for systems composed of PPG 400 + [Ch][Acetate] + H₂O and PPG 400 + [Ch]Cl + H₂O	87
C 2. Experimental binodal data for systems composed of K₂HPO₄ + [Ch][Acetate] + H₂O and K₂HPO₄ + [Ch]Cl + H₂O	88

List of figures

Figure 1. Structures of RuBisCO's forms I (a), II (b) and III (c). Adapted from Tabita et al. (17).	5
Figure 2. Scheme of the reactions chain catalyzed by RuBisCO in the Calvin-Benson-Bassham cycle. Adapted from Cummins et al. (19).	5
Figure 3. General scheme of the currently processes used in RuBisCO extraction.	9
Figure 4. General scheme of solid-liquid extraction applied to solid biomass samples.	11
Figure 5. Examples of cation structures of the most studied IL families. Adapted from Ferreira et al. (29)	13
Figure 6. Example of a binodal curve (black line) that fits experimental data (green squares) and a TL with 3 mixtures points (A, B and C).	15
Figure 7. Scheme of the extraction procedure proposed in this thesis.	17
Figure 8. Structures and abbreviations of the ILs applied in this work.	22
Figure 9. SDS-PAGE stained with BlueSafe. Effect of different aqueous solutions of ILs in the RuBisCO extraction from spinach using the following experimental conditions: IL concentration of 3.3 mM, 0.1 solid-liquid ratio, solid-liquid extraction during 30 min at 29 °C. Lane 1: Standard molecular weights; Lane 2: 1 mg/mL commercial RuBisCO, dissolved in PBS; Lane 3: extract with [Pr ₃ NC ₂ OC ₂][Sac]; Lane 4: extract with [Et ₃ NC ₂ OC ₂][Sac]; Lane 5: extract with [Et ₃ NC ₄ NC ₄][Br]; Lane 6: extract with [Bu ₃ NC ₄ NC ₄][Br]; Lane 7: extract with [MpyrNC ₄ NC ₄][Br]; Lane 8: extract with [MimNC ₄ NC ₄][Br]; Lane 9: extract with [Ch]Cl; Lane 10: extract with [C ₂ mim]Cl; Lane 11: extract with [C ₄ mim]Cl; Lane 12: extract with [C ₆ mim]Cl.	32
Figure 10. SE-HPLC spectra of aqueous solutions of synthesized ILs (A) and commercial ILs (B) after RuBisCO extraction from spinach leaves with an IL concentration of 3.3 mM.	33
Figure 11. RuBisCO's purity (%), orange line, and yield, green bars, after extraction from spinach leaves using different concentrations of IL (25 mM, 50 mM, 100 mM, 500 mM and 1 M), a solid-liquid ratio of 0.1 in a solid-liquid extraction during 30 min at 29 °C.	34
Figure 12. SDS-PAGE stained with BlueSafe. Effect of IL concentration in the RuBisCO extraction from spinach using the following experimental conditions: IL concentration of 25 mM – 1M, 0.1 solid-liquid ratio, solid-liquid extraction during 30 min at 29 °C. Gel A: Lane 1: Standard molecular weights; Lane 2: 1 mg/mL commercial RuBisCO, dissolved in PBS;	

Lanes 3 to 6: extracts with $[\text{Pr}_3\text{NC}_2\text{OC}_2][\text{Sac}]$ with the following order of concentrations: 25 mM; 50 mM; 100 mM and 500 mM; Lanes 7 to 10: extracts with $[\text{MpyrNC}_4\text{NC}_4]\text{Br}$ with the following order of concentrations: 25 mM; 50 mM; 100 mM and 500 mM; Lanes 11 to 15: extracts with $[\text{MimNC}_4\text{NC}_4]\text{Br}$ with the following order of concentrations: 25 mM; 50 mM; 100 mM; 500 mM and 1M. **Gel B:** Lane 1: Standard molecular weights; Lane 2: 1 mg/mL commercial RuBisCO, dissolved in PBS; Lanes 3 to 7: extracts with $[\text{Ch}]\text{Cl}$ with the following order of concentrations: 25 mM; 50 mM; 100 mM; 500 mM and 1 M; Lanes 8 to 12: extracts with $[\text{Ch}]\text{Br}$ with the following order of concentrations: 25 mM; 50 mM; 100 mM; 500 mM and 1 M. 35

Figure 13. RuBisCO's purity (%), orange line, and yield, green bars, after extraction from spinach leaves using different concentrations of IL (25 mM, 50 mM, 100 mM, 500 mM, and 1 M rpm), a solid-liquid ratio of 0.1 in a solid-liquid extraction during 30 min at 29 °C... 37

Figure 14. SDS-PAGE stained with BlueSafe. Effect of IL concentration in the RuBisCO extraction from spinach using the following experimental conditions: IL concentration of 25 mM – 1M, 0.1 solid-liquid ratio, solid-liquid extraction during 30 min at 29 °C. **Gel A:** Lane 1: Standard molecular weights; Lane 2: 1 mg/mL commercial RuBisCO, dissolved in PBS; Lanes 3 to 7: extracts with $[\text{Ch}][\text{DHP}]$ with the following order of concentrations: 25 mM; 50 mM; 100 Mm; 500 mM and 1 M; Lanes 8 to 12 extracts with $[\text{Ch}][\text{Acetate}]$ with the following order of concentrations: 25 mM; 50 mM; 100 mM; 500 mM and 1 M; Lanes 13 to 17 extracts with $[\text{Ch}][\text{DHC}]$ with the following order of concentrations: 25 mM; 50 mM; 100 mM; 500 mM and 1 M. **Gel B:** Lane 1: Standard molecular weights; Lane 2: 1 mg/mL commercial RuBisCO, dissolved in PBS; Lanes 3 to 7: extracts with $[\text{Ch}]\text{Cl}$ with the following order of concentrations: 25 mM; 50 mM; 100 mM; 500 mM and 1 M. 38

Figure 15. Response surfaces corresponding to the concentration of extracted RuBisCO (left) and yield of extraction (right) with the following combined parameters: (A) and (D) $[\text{Ch}][\text{Acetate}]$ concentration and pH; (B) and (E) $[\text{Ch}][\text{Acetate}]$ concentration and solid-liquid ratio; and (C) and (F) solid-liquid ratio and pH. 41

Figure 16. Response surfaces corresponding to the concentration of extracted RuBisCO (left) and yield of extraction (right) with the following combined parameters: (A) and (D) $[\text{Ch}]\text{Cl}$ concentration and solid-liquid ratio; (B) and (E) solid-liquid ratio and pH; and (C) and (F) $[\text{Ch}]\text{Cl}$ concentration and pH. 42

Figure 17. SDS-PAGE stained with BlueSafe. Lane 1: Standard molecular weights; Lane 2: 1 mg/mL commercial RuBisCO, dissolved in PBS; Lane 3: spinach extracts with [Ch][Acetate]; Lane 4: spinach extracts with [Ch]Cl; Lane 5: spinach extract with NH₄OH. 44

Figure 18. RuBisCO's yield, blue stroke, and RuBisCO's concentration, green bars, after extraction from spinach leaves at the optimal conditions and with NH₄OH, a solid-liquid ratio of 0.1 in a solid-liquid extraction during 30 min at 29 °C..... 44

Figure 19. ABS composed by PEG 1000+ spinach extract with [Ch][Acetate] (left) and PPG 400 + spinach extract with [Ch][Acetate] (right). 46

Figure 20. SE-HPLC spectra of the different extracts, phases and precipitates of the ABSs composed by IL and PPG 400, where (A) is for [Ch][Acetate] and (B) for [Ch]Cl. 47

Figure 21. ABS composed by K₂HPO₄ + spinach extract with [Ch][Acetate] (left) and K₂HPO₄ + spinach extract with [Ch]Cl (right). 48

Figure 22. SE-HPLC spectra of the different extracts, phases and precipitates of the ABSs composed by IL and K₂HPO₄, where (A) is for [Ch][Acetate] and (B) for [Ch]Cl. 49

List of tables

Table 1. Independent variables' coded levels applied in the factorial planning.	24
Table 2. Results of the extraction with [Ch][Acetate] at the optimal conditions.	41
Table 3. Results of the extraction with [Ch]Cl at the optimal conditions.	43

List of abbreviations

- [Bu₃NC₄NC₄]Br** - Tri(n-butyl)[4-butylamino-4-oxobutyl]ammonium bromide
- [C₂mim]Cl** - 1-ethyl-3-methylimidazolium chloride
- [C₄mim]Cl** - 1-butyl-3-methylimidazolium chloride
- [C₆mim]Cl** - 1-hexyl-3-methylimidazolium chloride
- [Ch][Acetate]** - Choline acetate
- [Ch][DHC]** - Choline dihydrogencitrate
- [Ch][DHP]** - Choline dihydrogen phosphate
- [Ch]Br** - Choline bromide
- [Ch]Cl** - Choline chloride
- [Cho][Pro]** – Choline proline
- [Et₃NC₂OC₂][Sac]** - Tri(ethyl)[2-ethoxy-2-oxoethyl]ammonium saccharinate
- [Et₃NC₄NC₄]Br** - Tri(ethyl)[4-butylamino-4-oxobutyl]ammonium bromide
- [MimNC₄NC₄]Br** - 1-(4-(butylamino)-4-oxobutyl)-1-methylimidazol-1-ium bromide
- [MpyrNC₄NC₄]Br** - 1-(4-butylamino-4-oxobutyl)-1-methylpyrrolidin-1-ium bromide
- [Pr₃NC₂OC₂][Sac]** - Tri(n-propyl)[2-ethoxy-2-oxoethyl]ammonium saccharinate
- [Pro][NO₃]** – Proline nitrate
- AAGB-IL** – Analogue of glycine-betaine ionic liquid
- ABS** – Aqueous biphasic system
- AGB-IL** – Glycine-betaine ionic liquid
- DTT** – Dithiothreitol
- HPLC** – High performance liquid chromatography
- IL** – Ionic Liquid
- LLE** – Liquid-liquid extraction
- PBS** – Phosphate buffer saline solution
- PEG 1000** – Polyethylene glycol with a molecular weight of 1000 g/mol
- PEG 400** – Polyethylene glycol with a molecular weight of 400 g/mol
- PEG 600** – Polyethylene glycol with a molecular weight of 600 g/mol
- PPG 400** - Polypropylene glycol with a molecular weight of 400 g/mol
- RSM** – Response surface methodology
- RuBisCO** – Ribulose-1,5-biphosphate carboxylase/oxygenase

SDS – Sodium dodecyl sulfate

SDS-PAGE – Sodium dodecyl sulfate polyacrylamide gel electrophoresis

SE-HPLC – Size-exclusion high performance liquid chromatography

SLE – Solid-liquid extraction

TL – Tie lines

TLL – Tie line length

Tris – tris(hydroxymethyl)aminomethane

List of symbols

K – Partition coefficient (dimensionless)

***R*²** – Correlation coefficient (dimensionless)

wt% - Weight percentage (%)

[RuBisCO] – Concentration of RuBisCO (mg/mL)

***EE*%** - Extraction efficiency (%)

1. Introduction

1.1. Scopes and objectives

The global population is increasing and, therefore, the search for new sources of protein is a demand (1,2). Proteins from green biomass are seen as an alternative in countries having the need to import them for feed and food production (1). In fact, it is possible to use green biomass, discarded by industries or biorefineries and from the waste of crops where the consumables are the fruits or roots, as a new protein source for both humans and animals (3,4). The crops' waste is the best source of green biomass, as these residues can be transported directly from the farm to the biorefinery. Furthermore, it can be a continuous source of green biomass since various crops are harvested at different times of the year. However, the efficiency of the methods used in protein recovery and their nutritional value maintenance are very important factors for the industries (5). Nowadays, it is already possible to extract proteins like RuBisCO with relatively high efficiency extraction and purity, using classical methodologies such as alkaline extraction, aqueous ammonia extraction, among others (5). Some authors have tried to develop an extraction method for RuBisCO, but have never achieved simultaneously a high extraction efficiency, a high purity or even a high specificity for RuBisCO (6,7). Nonetheless, its application in the food industry is not allowed due to the low value and concentration of the extraction product, the inefficient processing and the loss of insoluble proteins (3,7). RuBisCO is found at high concentrations in leaves (50 % - 60 % of total protein), which represents a great percentage of the green biomass (6,8–11). RuBisCO can be applied in several areas such as pharmaceutical, food and feed industries. However, its extraction and purification procedures have to be improved (1,3–7,9,12–14), in order to allow its widespread use.

Solid-liquid extraction with ionic liquids (ILs) combined with aqueous biphasic systems (ABS) seems a possible strategy to extract and then purify RuBisCO. The extraction of proteins with ILs maintaining their biological activity is already reported using ILs with high biocompatible and biodegradability (11,14,15).

Taking this into account, this work aims to use aqueous solutions of biocompatible ILs (derived from cholinium and glycine-betaine analogues) to extract RuBisCO from spinach (one of the most used plant for the development of extraction protocols and rich in RuBisCO) (1,2). Later on, the formation of ABS constituted by the same ILs, for RuBisCO purification is addressed. This investigation aspires to the development of a sustainable and, low-cost procedure for the extraction and purification of RuBisCO from spinach, allowing the

maintenance of protein structure and activity. Lastly, the major goal will be the replacement of spinach for any green biomass.

1.2. RuBisCO

1.2.1. Structure, characterization, and mechanisms of action

Ribulose-1,5-biphosphate carboxylase/oxygenase, RuBisCO (EC 4.1.1.39), is the most abundant protein (enzyme) in nature and it is present in a wide number of photosynthetic organisms such as plants, algae and various species of bacteria (3,8,9,11,12,16).

RuBisCO is present in nature in three different forms: I, II and III, as depicted in Figure 1 (8,17). The most common RuBisCO is the form I and it has 2 subclasses: green-type, present in proteobacteria, cyanobacteria, green algae and plants, and red-type, present in photosynthetic bacteria and nongreen algae. The form II occurs in dinoflagellates and bacteria and form III is exclusive of archaea (8,17).

Structurally, form I of RuBisCO consists of a hexadecameric complex, with about 550 kDa, and constituted by eight large subunits (RbcL, circa 50-55 kDa) and eight small subunits (RbcS, circa 12-18 kDa) (1,3,5,8,13,17). The complex's core is formed by a tetramer of two antiparallel dimers of RbcL, which have all the active sites of the enzyme, and RbcS are located in complex's borders (four RbcS in each top) (1,8,13,17). On the other hand, form II is constituted by one or more dimers of RbcL and form III has a ring shape formed by three to five dimers of RbcL and none of them have RbcS (8,17). Furthermore, form III has other functions besides being involved in photosynthesis, as D-ribulose-1,5-biphosphate (RuBP) regeneration produced in nucleotides metabolism (8).

RuBisCO has an isoelectric point between 4.6 and 5.5, varying with the species, a solubility above 80% at pH lower than 4 and higher than 6, and a denaturation temperature of 66.5 °C and 67.5 °C in alfalfa case and 64.9 °C for spinach RuBisCO (1,2,18).

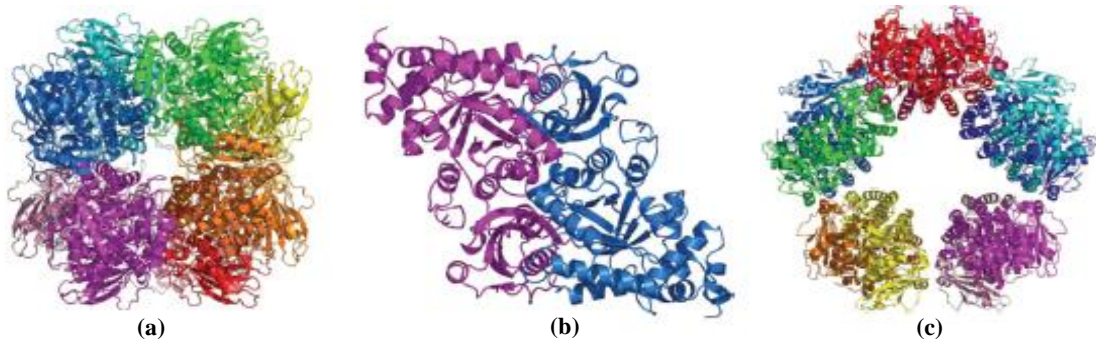


Figure 1. Structures of RuBisCO's forms I (a), II (b) and III (c). Adapted from Tabita et al. (17).

RuBisCO is the principal way to fixate atmospheric carbon in photosynthetic organisms (3,8,10,16,19). In this conversion, RuBisCO catalyses a chain of five reactions (Figure 2): the enolization of C3 from RuBP (RuBisCO's substrate); the carboxylation of C2 (CO₂ fixation); protonation of the bond established between the CO₂ and C2 which lead to C3 hydration and the cleavage of the C2-C3 bond of the unstable intermediate originating 2 molecules of 3-phosphoglyceric acid (3PGA) (8,16,19). 3PGA will enter in Calvin-Benson-Bassham cycle where it will be converted in glyceraldehyde-3-phosphate which is the predecessor of several biomolecules (sugars, fatty acids, and amino acids)(8).

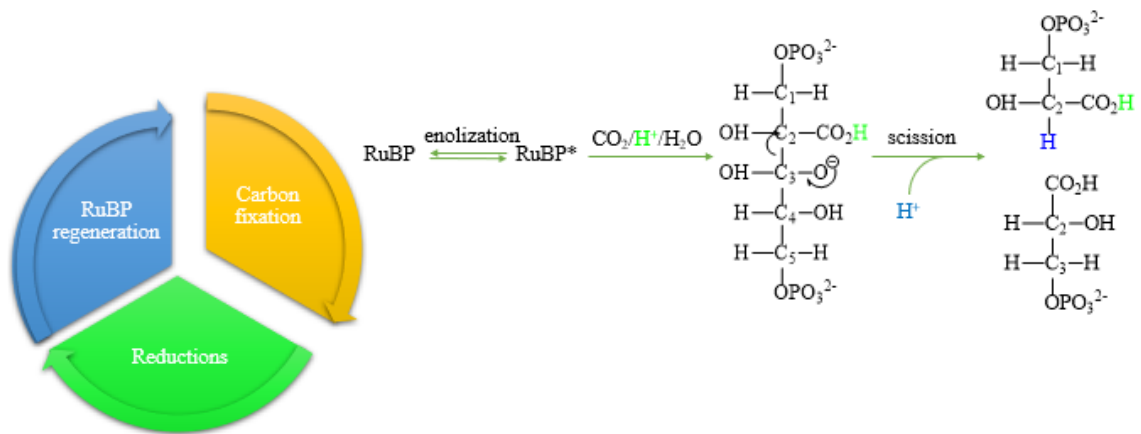


Figure 2. Scheme of the reactions chain catalyzed by RuBisCO in the Calvin-Benson-Bassham cycle. Adapted from Cummins et al. (19).

As previously mentioned, the complex composed by RbcLs have all the active sites of the enzyme, and presents a high structural stability and its sequence has circa of 60% of identity, meaning a relation between the complex structure and RuBisCO's performance (8). To RuBisCO be competent, Lys201 (on plants) must be carbamylated and then a Mg^{2+} will attach to this group, in order to RuBP bound in the active site (8,17). When RuBP linked to the active site, the flexible part of RuBisCO structure closes the active site, creating an interior space, allowing the electrophilic attack of RuBP from CO_2 or O_2 (8,17). Although RbcSs are in the extremities of Form I complex, they are needed for the enzyme to be functional and their sequence is more diversified and has more than 30% of identity. It was observed that both the subunits are affected by sulphur deficiency and cadmium stress (high concentration), although RbcL is more susceptible to cadmium presence and RbcS to sulphur deficiency since, if the plant has sufficient quantity of sulphur, the amount of RbcS increased in cadmium presence (20).

Organisms like plants and green algae have different families of RuBisCO's isoforms that have different expression rates affecting their catalytic activity and, it was though that RbcS emerge as an evolutionary adaptation to the increase of O_2 in the atmosphere (8). However, RuBisCO has three major questions affecting its role as CO_2 acceptor: efficiency related to the capability to accept O_2 , its reactions are error-prone and inhibitions (8–10,19). Regarding to the efficiency problem, RuBisCO only fixates two-five molecules of CO_2 per second in plants (it has a substrate-saturated K_{cat} in the range $1-12s^{-1}$ and a K_{cat}/K_C ratio in the range $2-40 \times 10^4 M^{-1}s^{-1}$ which is substantially lower than the ratios registered to other enzymes ($10^8-10^9 M^{-1}s^{-1}$)) (8,9). This disadvantage obligates the plant to produce large amounts of RuBisCO, representing in some cases, 50% of the total soluble protein in leaf tissues (6,8–11). However, these amounts of enzyme or the catalytic activity can be lower if the plant is in an environment with nitrogen deficiency or presence of cadmium (20,21). Furthermore, RuBisCO can accept O_2 , but the intermediate scission will produce only one molecule of 3PGA instead of two, and other of 2-phosphoglycolate (2PG) (8,9,19). This last one is toxic for chloroplasts and it can be converted in 3PGA by photorespiration (8). To avoid an unnecessary energy loss, CO_2 emission and disturbances in carbon and nitrogen cycles, some organisms developed strategies to concentrate CO_2 around RuBisCO like the existence of compartments with machinery for CO_2 concentration (for example carboxysomes in cyanobacteria and pyrenoids in green algae) (8,9). Nevertheless, CO_2 concentration affects

the RuBisCO's affinity by RuBP: in spinach, when the RuBP concentration is approximate to zero K_M is $1.5 \pm 0.5 \mu\text{M}$ and when concentration tends to infinite K_M is $0.8 \pm 0.2 \mu\text{M}$ (22). The second problem is related to the fact that reactions catalysed by RuBisCO are error-prone, as mention above. When errors occur, the intermediate is D-xylulose-1,5-biphosphate (XuBP) and the reactions products are D-glycero-2,3-pentodiulose-1,5-biphosphate (PDBP) and 2-carboxytetritol-1,4-biphosphate (CTBP). The formation of these sugar phosphates leads to enzyme inhibition since they had a strong affinity with RuBisCO's active site (8,10). In addition to the wrong protonation of the intermediate and the formation of sugar phosphates, RuBisCO can be inhibited for several reasons: with the bound of a RuBP uncarbamyated to the active site; the denominated autoinhibition which is the binding of RuBP to an uncarbamyated RuBisCO when the enzyme losses the ion Mg^{2+} from its active site in conjunction with the carbamyated group; and the production of 2'-carboxy-D-arabinitol-1-phosphate (CA1P) in plants in dark environment (8). In all these cases, the inhibition can be reverted by RuBisCO activase (Rca), which mediates RuBisCO's activity, with the exception in inhibition by sugar phosphates, were specific phosphatases must intervene for inhibitors degradation, which will later be converted in RuBP on Calvin-Benson-Bassham cycle (8,10,23).

1.2.2. RuBisCO's applications

RuBisCO can be applied in several fields, like food and feed industries, chemical industry, pharmaceutical, cosmetics, among others (1–7,9,12–14).

In animal feed, RuBisCO is already employed as a protein source through a white protein concentrate. The hydrolysis of this concentrate results in peptides with high solubility and nutritional value that can be incorporated in feed (12). However, in the food industry RuBisCO is not used yet, due to the extraction procedure applied, which leads to a lower quality than required because of polyphenols presence (12), and economic disadvantages (6). Nevertheless, many studies have been carried out for future applications, such as RuBisCO gels, products of thermal denaturation, which can be used in food formulation (13); undenatured RuBisCO to be applied in foaming, emulsifying and to form gels (13); peptides resulted from RuBisCO hydrolysis, which can be used in functional foods and nutraceuticals (3) and as additives (12), or simply as protein source (1). In fact, Martin et al. (1) investigated properties such as solubility, foam formation and stability, emulsion

formation and stability, water holding capacity, gelation and fracture properties of gels, and conclude that RuBisCO has the same or better results than soy and whey protein isolates.

For pharmaceutical and cosmetic industries, peptides resulted from the RuBisCO hydrolysis are the most desired due to their multiple properties, such as immunostimulant, antioxidant, opioid glucose uptake stimulant (5,12). Peptides like RuBisCO hydrolysate (with a degree of hydrolysis of 18.8%) can inhibit linoleic acid oxidation, ferric ion reduction, stabilization of 2,2'-azino-bis(3-ethylbenzothiazoline-6-sulfonic acid free radicals (ABTS^{*+}) (3).

Recently, artificial photosynthesis was developed and is about 12% more efficient and simpler compared to natural photosynthesis. Based on this information, Zhu et al. (24) immobilized RuBisCO in polydopamine-modified microfluidic reactors to produce glucose precursor. Their results are very promising because the immobilization improved the thermal and storage stabilities and at the end of 5 cycles. Moreover, RuBisCO had 90.4% of its initial activity and after 10 cycles, 78.5% of the initial activity was preserved. Furthermore, 3PGA production was continuous, if the injection of CO₂ and RuBP were constant and, in this way, the feedback inhibition was avoided, and the efficiency of the enzyme maximized (24).

1.3. RuBisCO extraction and purification methods

1.3.1. Traditional methods

The leaves used to extract and purify RuBisCO can be provided by biorefineries that discard higher amounts of green biomass or from crop residues (3,4). There are several methods of extraction such as percolation, maceration or Soxhlet extraction but commonly, RuBisCO and other intracellular leaf proteins are extracted through the same general procedure which involves four major steps (Figure 3): i) mechanical disintegration of the tissue, ii) protein solubilization, iii) protein precipitation and iv) protein concentration (3,4,10,25). Usually, the mechanical disintegration occur at pH 10-11 to promote, at the same time, the protein solubilization, while protein precipitation uses for pH treatment an acidic pH value (*e.g.* pH 3) at 4°C (3,10).

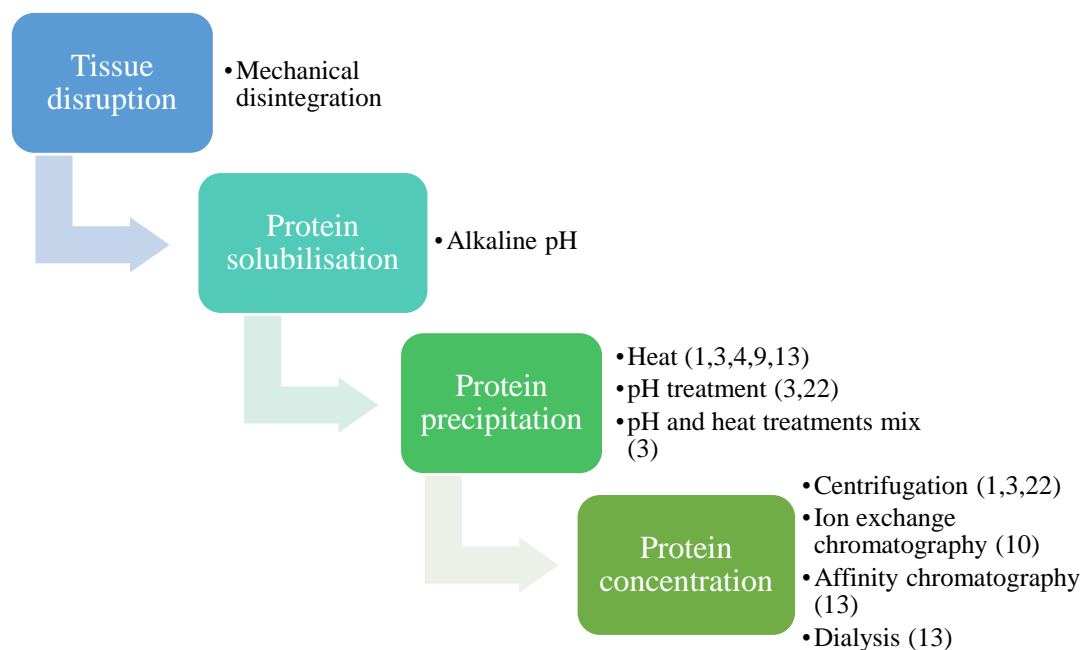


Figure 3. General scheme of the currently processes used in RuBisCO extraction.

From mechanical disintegration is obtained a green juice with soluble proteins, fibers, sugars, polyphenols and chlorophylls (6,12). Then, chlorophylls and fibers are removed by thermal precipitation, however fibers can retain water and, consequently, retain proteins with it (1,6,26). In order to recover the retained proteins in the precipitate, Tenorio et al. (6) tried to re-dissolve the proteins trapped in the precipitate with surfactants but failed in the improvement of the extraction efficiency of their procedure (mechanical disintegration followed by heating to 50°C and finishing with centrifugation). They obtained a solution with 41.1 wt% in protein content, and after a purification step, recovered 6% of RuBisCO with 90% purity. During thermal precipitation, depending on temperature, can also occur protein denaturation. Due to ionic bonds cleavage, the release of divalent anions and the capture of divalent cations, protein gelation resulted from the aggregation of denatured proteins when the concentration of proteins is higher than the percolation limit (13). Since polyphenols at alkaline pH are highly reactive with hydroxyl and aromatic groups from proteins (creating cross-linked between proteins and oxidized polyphenols (4)) and sugars, causing a brown coloration to the solution resulted from their oxidation, they have to be removed after mechanical disintegration, to avoid a decrease on the final product quality (12). For example, France – Luzerne (12) produced a white protein concentrate allowed to be used in feed but not in food industry because of phenolic compounds presence. To remove

them, without changing the nutritional value and the functional properties of the final product, ultrafiltration was introduced in the protocol but with no significant decrease in the polyphenol's concentration and the color intensity. To improve these results, ultrafiltration was conjugated with sorption techniques and the best result was with a polystyrene resin where the polyphenols decreased 94% (12).

This general procedure with 4 major steps is the most relevant due to its high extraction efficiencies, but there are other protocols, like alkaline extraction (5). As an alkaline extraction example, Zhang et al. (7) used a conjugation of heat and pH treatment to extract all the proteins in leaves and they were able to extract 95% of total protein content in 4 h at 95°C with a v/w of 40 mL/g NaOH 0.1M (pH 3.5), where 85% of the protein has 52% purity. Nevertheless, this procedure does not have the efficiency needed to be executed on a large scale.

Kobbi et al. (3) also studied the feasibility and efficiency of ammonium hydroxide and protein precipitation at pH 3 without prejudice the biological activity. They were able to remove 80% of polyphenols and extract RuBisCO with around 90% of purity. Furthermore, comparing their results with commercial products, there are no significant differences between them.

The application of methods with extreme conditions such as alkaline pH, the use of organic solvents and high temperatures improve the extractions of these biomolecules, although it leads to protein activity loss (6). Therefore, other techniques have been applied for the RuBisCO extraction and purification like crystallization, aqueous biphasic systems (ABS), pulsed electric fields, extraction with ionic liquids, ultra-sonification, microwaves, among others (4), to improve the extraction yields.

1.3.2. Solid-liquid extraction

1.3.2.1. General concepts

Solid-liquid extractions (SLE), one of the oldest unit operations in the chemical industry, is another possible approach to extract RuBisCO from biomass. This type of extraction allows soluble components to be removed from solids using a solvent, where operational conditions such as temperature, extraction time, and solid-liquid ratio are optimized, with subsequent separation of the phases by decantation, filtration or centrifugation (Figure 4).

The selection of the solvent is carried out taking into consideration its selectivity, capability for dissolving the solute, density, viscosity, surface tension, toxicity, boiling temperature, chemical and thermal stabilities and cost (27). Obviously, due to the toxicity of some organic solvents, there are some restrictions to their use in the food, cosmetic and pharmaceutical industries (27). Furthermore, the organic compounds commonly employed display major drawbacks in what concerns safety and environmental issues.

In summary, SLEs involves the extraction and dissolution of a given compound from a solid matrix in a given solvent and without the identification of selective solvents, extractions from biomass usually result in a complex extract (28). An example is the extraction used to extract the leaf proteins (including RuBisCO), described in Section 1.3, where the SLE is the combination of the two first steps: the mechanical disintegration and protein solubilization. Therefore, after the extraction step, induced precipitation, distillation, and chromatography, among others, are used as separation/purification techniques. Most of these techniques generally involve the use of volatile and often toxic organic solvents, additionally leading to environmental and human concerns (28). Furthermore, the costs associated with the final product are strongly dependent on the downstream processing, namely the type of techniques used and the number of steps required (28). Thus, it is of crucial relevance to explore alternative solvents environmentally friendly and develop cost-effective and sustainable extraction and purification techniques, which could be ideally incorporated in an integrated process. A possible alternative includes the separation and purification of the target compounds from complex extracts using liquid–liquid extractions (LLE).

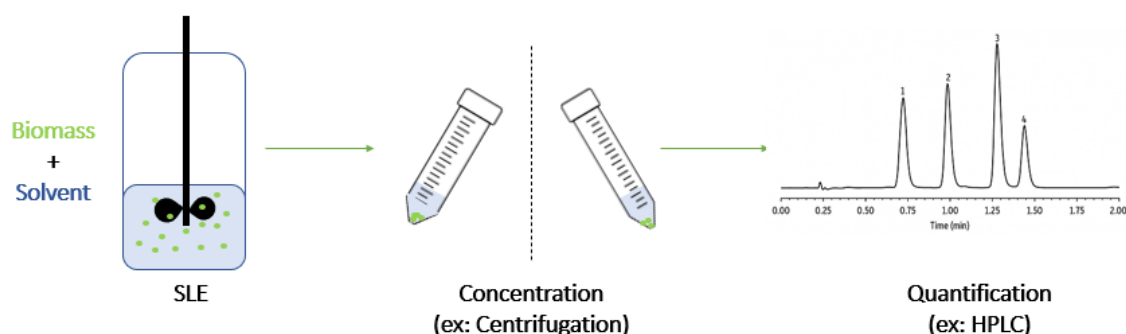


Figure 4. General scheme of solid-liquid extraction applied to solid biomass samples.

1.3.3.2. Solid-liquid extraction using Ionic Liquids

ILs are ionic compounds with fusion temperatures lower than 100°C, because of the lack of an ordered crystalline structure (11,14,29). Usually, they are constituted by a large organic cation and an organic or inorganic anion (Figure 6). Due to these characteristics, they have a negligible vapor pressure, a high chemical and thermostability, ionic conductivity non-inflammable and are liquid in a wide range of temperatures (11,29). These characteristics make ILs a good alternative to organic solvents. The first IL was developed in 1914 and one of the firsts applications was its use as a solvent to store and preserve cellulose and then its application in aluminium electrodeposition (29,30). In 1992, ILs stable at air and water presence were developed with other cations, as imidazolium (29), to prevent denaturation. Divya et al. (31) proved that imidazolium-based ILs prevent protein aggregation and unfolding with an increase in thermal stability. However, imidazolium present some toxicity and is why other authors like, Sahoo et al. (32) studied cholinium-based ILs for the same purpose of Divya et al. (31) and concluded that solutions with a low concentration of choline proline ([Ch][Pro]) and proline nitrate ([Pro][NO₃]) preserve the cytochrome-c tertiary structure.

However, the major benefit in use ILs comes from the possibility to change one or the two ions of the IL, tuning its hydrophobicity, polarity, and viscosity (11,29).

ILs have been used in the SLE of several biomolecules with interesting results that support its application instead of organic solvents. As examples, Martins et al. (15) extracted phycobiliproteins with ionic liquid aqueous solutions. They improved extraction by 46,5 % with a purity similar to other procedures (like solid-liquid extraction, enzymatic process, etc) without compromising the secondary structure of the protein; Cláudio *et al.* (33) extracted caffeine with a yield up to 9 wt% per guaraná dry weight at 70 °C for 30 min with the confirmation that the IL solutions are recyclable and reusable and, Martins *et al.* (34) developed a cost-effective and efficient process for chlorophylls that allowed the maintenance of the stability of the final product for more than a month.

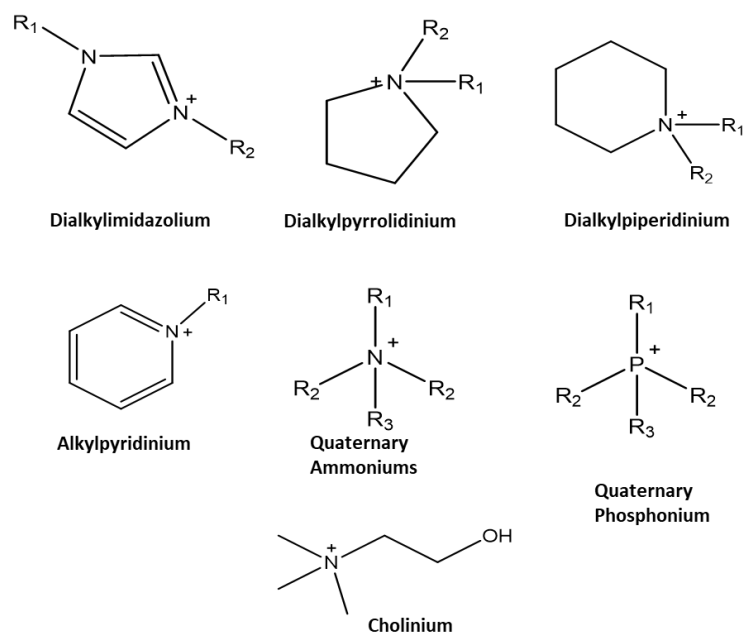


Figure 5. Examples of cation structures of the most studied IL families. Adapted from Ferreira et al. (29)

1.3.3. Aqueous Biphasic Systems (ABS)

1.3.3.1. General concepts

LLE is usually performed using organic solvents immiscible with water (35). Compared to chromatography, liquid-liquid systems offer technological simplicity and low cost, as well as the capability to provide high yields, improved purification factors, enhanced selectivity and the possibility of combining the recovery and purification steps (35). Aiming at avoiding the use of organic solvents in LLE, in 1958, Albertsson introduced the aqueous biphasic systems (ABS) for the separation of (bio)molecules by their partitioning between two liquid aqueous phases (36). ABS are good alternatives for the purification of several (bio)molecules because of their simplicity, low cost, the possibility to use components non-inflammable, non-volatile and with low toxicity. Moreover, they can be improved to separate multiple products and are easy to scale-up (14,29,37–39). This type of liquid-liquid extraction method can combine the separation and purification in just one step (29,39).

ABS are composed by two incompatible solutes, above certain conditions (temperature, concentration, etc), like two polymers or salts, or one polymer and one salt. ABS's phases have a high content in water, creating biocompatible systems (11,14,29,37–39).

The prediction of an ABS formation (Figure 5) is based on their binodal curve, which separates the monophasic (below the curve) and the biphasic regions (above the curve). In the biphasic region, the mixture of the two compounds forms an ABS, and the larger the area of the biphasic region the greater the capability to form an ABS (29). Empirically, binodal curves can be determined by several methods (40), nevertheless, cloud point titration and turbidimetric method are simpler since the systems' compositions are determined by weight quantification (41,42). For the cloud point titration method, the salting-out agent solution is added dropwise to the solution of the second constituent until obtaining a cloudy solution and, at this point, the salting-out agent solution is replaced by water until the cloudy solution becomes clear and this procedure is repeated until the solution loses the capability to become cloudy or clear (41,43). In the turbidimetric method case, several mixture points are made in the biphasic region, and water is added dropwise until the solution becomes clear (42).

Additionally, to characterize the ABS, the tie-lines (TLs) can be determined, which provide information about the composition of each phase. To this end, a mixture point in the biphasic region is selected (with a precise quantity of each compound) and, after the formation of the biphasic system, both phases are separated and weighted and with their weight percentage, and using an appropriate software, a line is drawn, intersecting the mixture point and the binodal curve in two points (TL) (44). The two intersections points between the binodal curve and the TL gives the composition of each phase and the phases of every mixture points that coincide with that TL have the same composition but different phase volumes, as represented in Figure 5 (29,44). The length of the TL (TLL) is used as an indicator of the differences between the compositions of the phases and enables to predict the product partition. It is possible to have a TLL of zero and in this case, the mixture point is known as critic point and the bottom and top phases have the same compositions (29).

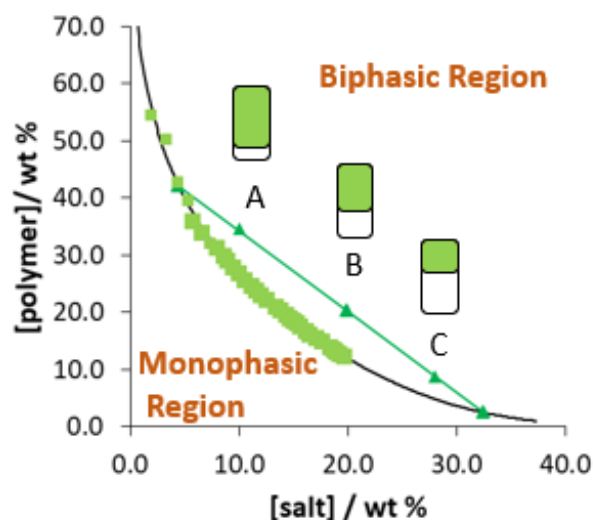


Figure 6. Example of a binodal curve (black line) that fits experimental data (green squares) and a TL with 3 mixtures points (A, B and C).

The extraction of solutes in ABS can be evaluated by the partition coefficient (K) and extraction efficiency (EE%) of the solute, which quantifies the solute distribution between both phases of the ABS (39) and between each phase and the total mixture (14,38,45), respectively. K is the ratio between the solute concentration in both phases and, in a case where K is determined in function to top phase, if K is lower than 1, the product of interest is major present in the bottom phase, and if K is higher than 1, most of the product of interest is in the top phase. A K value close to 1, means that the product of interest has partitioned similarly between the two phases (39). The partition of the product of interest is highly dependent on the affinity between the product and the phase component and physicochemical parameters such as pH, temperature, and TLL (11).

Nowadays, it's possible to recover products using conventional ABS (polymer-based ABS), with yields between 65 and 100 %, from different sources, like biologic suspensions, fermentation broths, etc (29,39,46). However, the conventional ABS presents some disadvantages, like viscosity, opacity and a limited range of polarity (37). So as alternatives to polymers and salts, ionic liquids (ILs) have emerged, and combinations between ILs and polymers/amino acids/ carbon hydrates have been used today (29,39).

1.3.3.2. Ionic liquid-based ABS (IL-based ABS)

Nowadays, ILs are used as solvents in chemical reactions, synthesis, chromatography and liquid-liquid extractions of biomolecules from water solutions through the ABS formation and the application of hydrophobic or hydrophilic ILs (29). As referred previously, ABS can be formed by the conjugation of ILs with other compounds (polymers, salts, etc.) (11,29). These ABS had advantages compared to the conventional ones, since ILs can be designed according to the final purpose of the work. Moreover, the lower viscosity of IL-based ABS leads to a quicker phase separation and higher extractions efficiencies (29).

Several biomolecules, including amino acids (47–49), proteins (50,51), and antibiotics like tetracycline and ciprofloxacin (52) have been extracted with IL-based ABS with extraction efficiencies close to 100%.

RuBisCO extraction with IL-based ABS was already studied. Ruiz et al. (14) compared a polymer-salt ABS (PEG 400 - Potassium citrate), a polymer-IL (PEG 400 - Cholinium dihydrogen phosphate) and an IL-salt ABS (Iolilyte 221PG - Potassium citrate). PEG was chosen because of its capacity to stabilize proteins, Iolilyte 221PG because of its higher capability to form ABS and cholinium-based ILs because they had buffer properties, low toxicity, are biodegradable, low cost and maintain the protein structure and biological activity (11,14). Ruiz et al. (14) concluded that ABS with Iolilyte 221PG had a better extraction efficiency, 98.8% by a single extraction, in comparison to the 96.6 % for PEG 400 – Potassium citrate and the 79.6 % for PEG 400 - Cholinium dihydrogen phosphate. However, the ABS with PEG 400 preserve the protein integrity so, with no surprise, they observed that RuBisCO migrate to PEG-rich phase. Contrarily, in the ABS with Iolilyte 221PG occur formation of aggregates and they noticed that the increase of IL concentration affects protein stability.

Desai et al. (11) also report the RuBisCO migration to Iolilyte 221PG-rich phase and Iolilyte 221PG-sodium potassium buffer with a K 3-4 times higher than the K registered to PEG-potassium citrate. However, with the increase of IL concentration, RuBisCO began to aggregate and fragment.

Due to these results and their natural origin glycine-betaine ILs (AGB-ILs) are an alternative for the extraction and purification of RuBisCO. Betaine is a methyl derivative of glycine and is present in biologic fluids, plants, microorganisms, among others when the cells are exposed to a stress environment (53). Pereira et al. extracted 5 amino acids with

ABSs composed by salt and analogues of glycine-betaine ILs (AAGB-IL) and extracted 65% to 100% in just one step. AAGB-ILs with hydrophobic properties were already used in pesticides and metallic ions extraction (53,54). Furthermore, Capela et al. (55) were able to extract monoclonal antibodies with ABSs composed by AAGB-ILs with recovery yields up to 100% and a purification factor up to 1.6 preserving, at the same time, the biological activity of the biomolecule.

1.4. Main goal of the thesis

Because of the high costs, time or complexity of various processes, integrated processes began to be developed and consists of the combination of several unit processes at the same equipment (56). One of the purposes of this thesis is the development of an integrated process where in the first step occur the RuBisCO's SLE and in the second and last step, through the addition of a second compound, is formed an ABS for the separation and purification of the enzyme. The application of aqueous solutions of ILs in the SLE allows a more selective extraction of RuBisCO thanks to some of the characteristics of ILs (such as the capability to change one of the ions) and allying to the high extraction efficiencies of IL-based ABSs it is possible the development of a more selective extraction procedure for RuBisCO. For this thesis the chosen ILs are cholinium- and AGB-based, increasing the interest of this alternative because beyond the selectivity, this procedure will be biodegradable with low toxicity and cost.

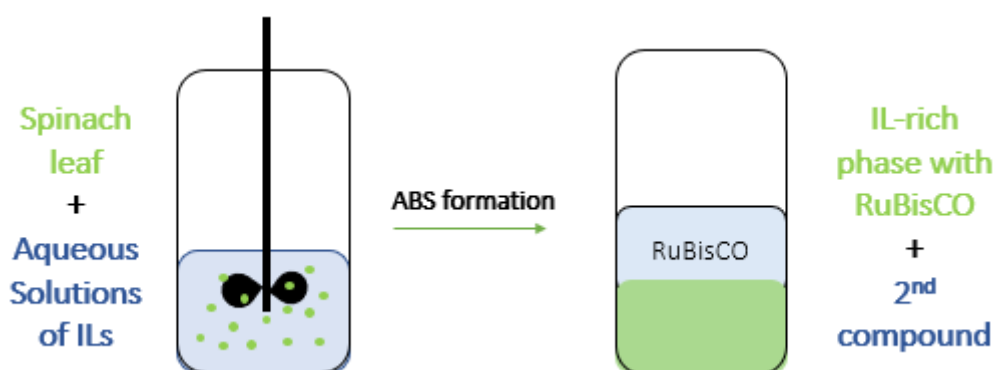


Figure 7. Scheme of the extraction procedure proposed in this thesis.

2. Experimental Section

2.1. Materials

RuBisCO was extracted from spinach (ready to cook) acquired in a local supermarket, at Aveiro. RuBisCO standard (D-Ribulose 1,5-diphosphate carboxylase from spinach) and phosphate buffered saline (PBS) were purchased from Sigma-Aldrich. The solvent applied in the conventional extraction method of RuBisCO used was ammonium hydroxide (NH₄OH, 25% of purity, Fluka). In the SLE were used the following ILs (Figure 8): choline chloride ([Ch]Cl, 98 % of purity, Acros Organics), choline bromide ([Ch]Br, > 98 % of purity, TCI), choline acetate ([Ch][Acetate], > 99 % of purity, Iolitec), choline dihydrogencitrate ([Ch][DHC], 99 % of purity, Sigma-Aldrich) and choline dihydrogen phosphate ([Ch][DHP], > 98 % of purity, Iolitec); 1-ethyl-3-methylimidazolium chloride ([C₂mim]Cl, 98 % of purity, Iolitec), 1-butyl-3-methylimidazolium chloride ([C₄mim]Cl, 99 % of purity, Iolitec), 1-hexyl-3-methylimidazolium chloride ([C₆mim]Cl, 98 % of purity, Iolitec); and the AGB-ILs, tri(n-propyl)[2-ethoxy-2-oxoethyl]ammonium saccharinate ([Pr₃NC₂OC₂][Sac], > 98 % of purity), tri(ethyl)[2-ethoxy-2-oxoethyl]ammonium saccharinate ([Et₃NC₂OC₂][Sac], > 98 % of purity), tri(ethyl)[4-butylamino-4-oxobutyl]ammonium bromide ([Et₃NC₄NC₄]Br, > 98 % of purity), 1-(4-butylamino-4-oxobutyl)-1-methylpyrrolidin-1-ium bromide ([MpyrNC₄NC₄]Br, > 98 % of purity), 1-(4-(butylamino)-4-oxobutyl)-1-methylimidazol-1-ium bromide ([MimNC₄NC₄]Br, > 98 % of purity), tri(n-butyl)[4-butylamino-4-oxobutyl]ammonium bromide ([Bu₃NC₄NC₄]Br, > 98 % of purity). AGB-ILs were synthesized and kindly supplied by Professor Aminou Mohamadou from Institut de Chimie Moléculaire, Université de Reims Champagne-Ardenne.

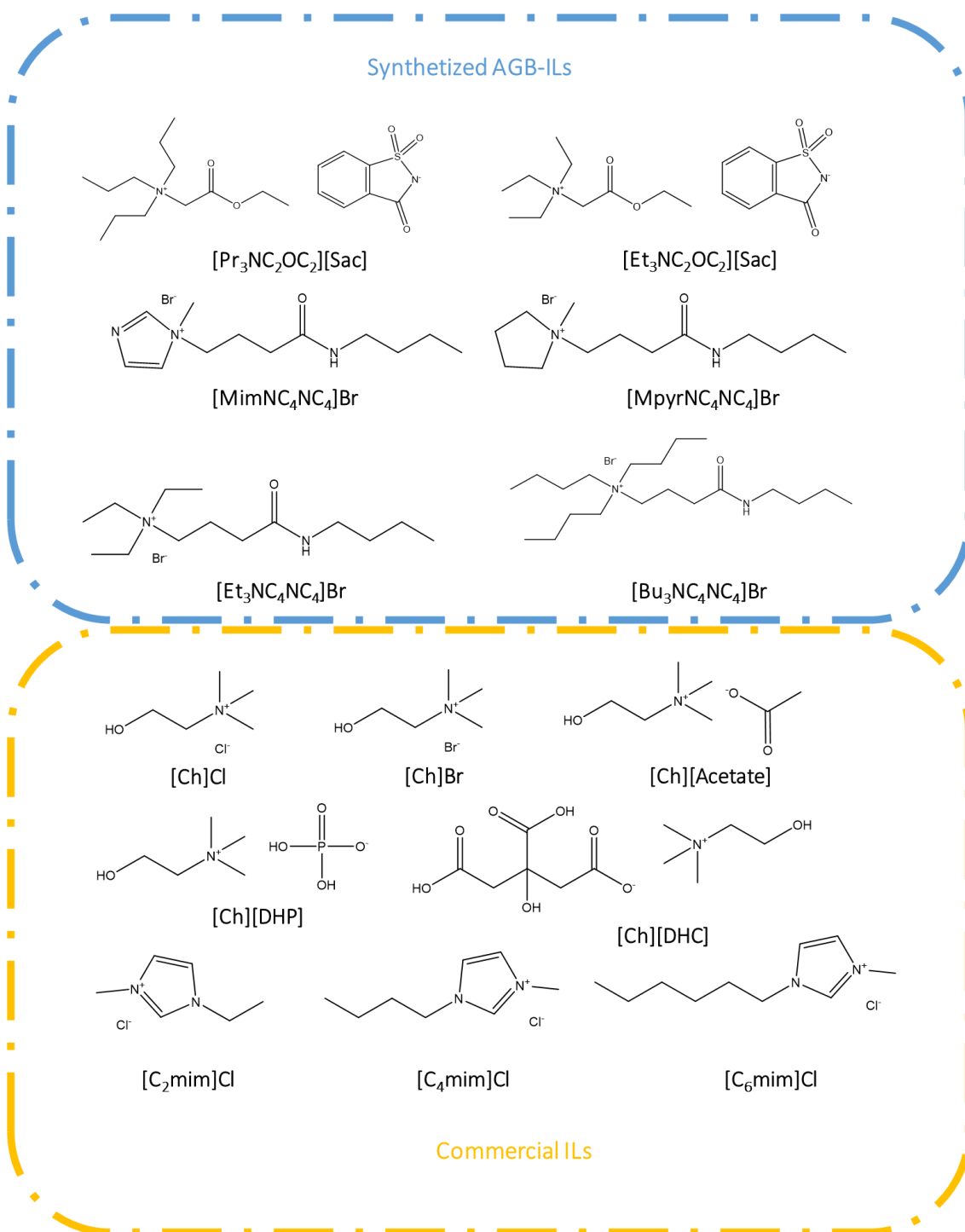


Figure 8. Structures and abbreviations of the ILs applied in this work.

To perform sodium dodecyl sulphate polyacrylamide gel electrophoresis (SDS-PAGE) were used: tris(hydroxymethyl)aminomethane (Tris, PA, Pronalab), sodium dodecyl sulfate (SDS, 99 % of purity, Acros Organics), glycerol (99 % of purity, Acros Organics), bromophenol blue (pure, Merck), dithiothreitol (DTT, 99 % of purity, Acros Organics),

RunBlue 20x SDS run buffer TEO – Tricine – SDS (Expedeon), RunBlue SDS Gel 4-12%, 12 wells, GRS Protein Marker MultiColour (gris Research Solutions), and BlueSafe (nzytech).

For size-exclusion high-performance liquid chromatography (SE-HPLC) quantification it was used sodium phosphate dibasic heptahydrate ($\text{Na}_2\text{HPO}_4 \cdot 7\text{H}_2\text{O}$, 98.0-102.0 % of purity, Sigma-Aldrich), sodium dihydrogenphosphate (NaH_2PO_4 , 99 % of purity, Sigma-Aldrich) and sodium chloride (NaCl , 99.5 % of purity, Panreac).

To form the ABSs it was used polypropylene glycol 400 $\text{g}\cdot\text{mol}^{-1}$ (PPG 400), polyethylene glycol 1000 $\text{g}\cdot\text{mol}^{-1}$ (PEG 1000), both from Sigma Aldrich, and di-potassium hydrogen phosphate trihydrate ($\text{K}_2\text{HPO}_4 \cdot 3\text{H}_2\text{O}$, 98% of purity, Scharlau).

2.2. RuBisCOs' solid-liquid extraction

Fresh spinach leaves were stored at $-80\text{ }^\circ\text{C}$ and exactly before the extraction were ground with liquid nitrogen in a mortar. The RuBisCOs' extractions were carried out in a Carrousel from *Radleys Tech* able to both stir and maintain the temperature within $\pm 0.5\text{ }^\circ\text{C}$. The experimental conditions were adapted from Leite *et al.* (57). All the experiments were performed at 600 rpm, $(29.0 \pm 0.5)\text{ }^\circ\text{C}$ for 30 min with a 0.1 solid-liquid ratio. The aqueous solutions containing known amounts of IL and biomass were prepared gravimetrically within $\pm 10^{-4}\text{ g}$. The impact of different concentrations of IL and pH in the extraction of RuBisCO were studied. For each set of conditions were prepared three replicas and the extractions evaluated by SDS-PAGE and HPLC quantification. After the extraction, the solutions were centrifuged (at 7000 rpm for 30 min in a *Neya 16R* centrifuge) to separate the extracts from biomass. The pH of the extracts was measured at $(25.0 \pm 0.1)\text{ }^\circ\text{C}$ with a *Metrohm 827 pH lab* equipment.

2.3. Response surface methodology (RSM)

In order to analyse several operational conditions and identify the most significant parameters in RuBisCOs' extraction, a response surface methodology was applied. In a 2^k RSM, k are the factors that provide a different response and through the adjustment of the data to a second order polynomial equation (Equation 1):

$$y = \beta_0 + \sum \beta_i X_i + \sum \beta_{ii} X_i^2 + \sum_{i < j} \beta_{ij} X_i X_j \quad (1)$$

where y is the response variable, β_0 , β_i , β_{ii} and β_{ij} are the adjusted coefficients for the intercept, linear, quadratic and interaction terms, respectively, X_i and X_j are independent variables. The analysis of the surface response curves resulted from this method, leads to the determination of the optimal conditions.

After the initial screening using different ILs, [Ch]Cl and [Ch][Acetate] showed to be the best option as solvents to optimize extraction of RuBisCO from spinach leaves. Operational conditions, namely, pH, solid-liquid ratio and IL concentration were optimized by a 2^3 factorial planning to simultaneously analyse various operational conditions and to identify the most significant parameters that enhance the extraction yield and the extracted concentration of RuBisCO. The remaining extraction conditions used were the same as the SLE extraction protocol described in section 2.2.

The 2^3 factorial planning is defined by the central point (level zero), the factorial points (1 and -1, level one) and the axial points (level α), see Table B 1 in Appendix B. The independent variables coded levels used in the factorial planning are presented in Table 1. The axial points are encoded at a distance α from the central point (58):

$$\alpha = (2^k)^{1/4} \quad (2)$$

Table 1. Independent variables' coded levels applied in the factorial planning.

Studied parameters	Level				
	Axial -1.68	Factorial -1	Central 0	Factorial 1	Axial 1.68
pH	2.8	4.5	7.0	9.5	11.20
Solid-liquid ratio	0.02	0.050	0.100	0.150	0.184
Concentration (M)	0.323	0.800	1.500	2.200	2.676

The obtained result was statistically analysed with a 95 % confidence level and a student t-test was applied to verify the statistical significance of the adjusted data (Appendix B, Table B 4.1 – Table B 5.2). The regression coefficient (R^2), the lack of fit and the F-value obtained from the analysis of variance (ANOVA) were evaluated to determine the adequacy

of the model. The Statsoft Statistica 10.0[®] software was used in all statistical analyses and to drawing the response surfaces. Contour plots of the yield of extraction and of the extracted concentration of RuBisCO were generated from adjusted models, and through their analysis, the optimal conditions can be determined.

2.4. SDS-PAGE analysis

The proteins profile of the obtained extracts was determined by SDS-PAGE. The samples were diluted at a 1:1 (v/v) ratio in a sample buffer composed by 2.5 mL of 0.5 M Tris-HCl pH 6.8, 4.0 mL of 10 % (w/v) SDS solution, 2.0 mg of bromophenol blue, 2.0 mL of glycerol and 310 mg of DTT. After this dilution, the samples were heated for 5 min at 95 °C, to break up the quaternary structure and deconstruct part of the tertiary structure by reducing the disulfide bonds and denaturing the proteins. All samples were loaded and run on a polyacrylamide gel (stacking: 4 % and resolving: 20 %). To stain the proteins, the gels were impregnated with BlueSafe and stirred in an Heidolph[™] rotamax 120 orbital shaker at 50 rpm for 40 minutes at room temperature. GRS Protein Marker MultiColour (grisip Research Solutions) was used as molecular weight standards while commercial RuBisCO from spinach (Sigma-Aldrich) was used as RuBisCO standard.

2.5. SE-HPLC analysis

Protein quantification was performed by size-exclusion high-performance liquid chromatography (SE-HPLC). A calibration curve was determined for this purpose (Appendix A, Figure A 2) using commercial RuBisCO from spinach (Sigma-Aldrich).

A phosphate buffer solution (1000 mL), used as mobile phase, was prepared using 47 mL of a Solution A (27.8 g of NaH₂PO₄), 203 mL of a Solution B (53.65 g Na₂HPO₄•7H₂O) and 17.5 g of NaCl. Each sample was diluted at a 1:9 (v/v) ratio in the phosphate buffer and then injected on a *Chromaster HPLC system (VWR Hitachi)*. The SE-HPLC was performed on an analytical column *Shodex Protein KW-802.5 (8 mm x 300 mm)*. The mobile phase, a 50 mM phosphate buffer + NaCl 0.3 M, ran isocratically with a flow rate of 0.5 mL/min and the injection volume was 25 µL. The column oven and autosampler temperatures were kept at 40 °C and at 10 °C, respectively. The wavelength was set at 280 nm using a DAD detector. The obtained chromatograms were treated and analysed using the PeakFit version 4 software.

The purity and yield of RuBisCO were calculated based on Equations 3 and 4, respectively. The purity (%Purity, Equation 3) was determined by the ratio between the peak area of RuBisCO ($A_{RuBisCO}$) and the area of all peaks of the chromatogram, corresponding to other proteins present in the samples (A_{Total}). The yield (Equation 4) was calculated by the ratio between the concentration of RuBisCO in the extract ($C_{extract}$) and the biomass mass ($m_{biomass}$).

$$\%Purity = \frac{A_{RuBisCO}}{A_{Total}} \times 100 \quad (3)$$

$$Yield = \frac{C_{extract}}{m_{biomass}} \quad (4)$$

2.6. RuBisCOs' purification using ABS

The extract containing RuBisCO, other biomolecules and IL was used to form the ABS. Additionally, from the phase diagrams determined by Pereira et al. (59), ternary mixtures composed of IL + PPG 400 (15 wt% of [Ch][Acetate] + 19 wt% of water + 67 wt% of polymer and 12 wt% of [Ch]Cl + 21 wt% of water + 67 wt% of polymer) and IL + PEG 1000 (15 wt% of [Ch][Acetate] + 19 wt% of water + 67 wt% of polymer and 12 wt% of [Ch]Cl + 21 wt% of water + 67 wt% of polymer), which lead to the formation of two-phase systems, were chosen to carry out the separation and purification of RuBisCO. Other ABSs composed by IL+salt were studied. The ternary mixtures were selected from the phase diagrams of [Ch][Acetate] + K_2HPO_4 (27 wt% of IL + 44 wt% of water + 29 wt% of salt) and [Ch]Cl + K_2HPO_4 (24 wt% of IL + 48 wt% of water + 29 wt% of salt) determined by Belchior *et al.* (60) and Osloob *et al.* (61) respectively. Each mixture was stirred, centrifuged for 15 min at 4000 rpm to reach the biomolecules equilibrium and partition between the coexisting phases. After a careful separation of the phases, RuBisCO present in each phase was quantified by SE-HPLC and the protein profile was analysed by SDS-PAGE. At least three independent ABS were prepared, and three samples of each phase were quantified. Control or “blank” solutions at the same mixture point used for the extraction studies (with no biomolecules) were used in all systems

The partition coefficient (K), the yield of extraction and the extraction efficiency ($EE\%$) of each system to RuBisCO were defined by Equations 5 to 7. The equations are written for the ABS with PPG 400, where most of the enzyme has partitioned for the bottom phase. For the ABS with K_2HPO_4 , Equation 5 is inverted and in Equations 6 and 7, the numerator is related to the top phase instead of the bottom.

$$K = [RuBisCO]_{bottom}/[RuBisCO]_{top} \quad (5)$$

$$Yield (\%) = ([RuBisCO]_{bottom}/[RuBisCO]_{ABS}) \times 100 \quad (6)$$

$$EE\% = (m_{RuBisCO_{bottom}}/(m_{RuBisCO_{top}} + m_{RuBisCO_{bottom}})) \times 100 \quad (7)$$

3. Results and Discussion

3.1. RuBisCOs' solid-liquid extraction

In general, the extraction methods applied in the protein extraction of green biomass involves the use of organic solvents with extreme temperatures or pH and sometimes the combination of both. These conditions can able the extraction but with the cost of the protein activity loss (6). ILs have been used in the SLE of several biomolecules, such as proteins (15), caffeine (33) and chlorophylls (34) with interesting results that support its application instead of organic solvents.

3.1.1. Effect of aqueous solutions of ILs on the RuBisCO's extraction

In this work, for RuBisCO extraction from spinach, the effect of aqueous solutions of biocompatible glycine-betaine- ILs, cholinium- and imidazolium-based ILs was firstly addressed in order to select the most promising ILs. Specifically, the ILs used were: [Et₃NC₄NC₄]Br, [MpyrNC₄NC₄]Br, [MimNC₄NC₄]Br, [Bu₃NC₄NC₄]Br, [Pr₃NC₂OC₂][Sac], [Et₃NC₂OC₂][Sac], [Ch]Cl, [C₂mim]Cl, [C₄mim]Cl and [C₆mim]Cl (Figure 8). The operational conditions were adapted from Leite et al. (57) and kept constant in all the experiments, namely the IL concentration of 3.3 mM, the solid-liquid ratio of 0.1 and the extraction time of 30 min and temperature at 29 °C. After the extraction, all extracts were analysed by SDS-PAGE (Figure 9) and SE-HPLC (Figure 10).

The electrophoresis (Figure 9) demonstrates, by the presence of the large subunit (~55 kDa) and small subunits (12-18 kDa) of RuBisCO, that all ILs are capable to extract RuBisCO, from spinach. However, depending on the IL the intensity of the large subunit is distinct revealing the different performance of all ILs. [Et₃NC₂OC₂][Sac] (Figure 9, lane 4) is the IL with the lower capacity to extract RuBisCO, since presents a less intense bands around 55 kDa. On the other hand, [Pr₃NC₂OC₂][Sac], [Ch]Cl and [C₂mim]Cl (Figure 9, lanes 3, 9 and 10, respectively) are the most promising ILs. Comparing the results obtained with the imidazolium-based ILs, it's it possible to conclude that all of them extracted RuBisCO but the increase of the carbon chain length decreases the extraction yield due to the intensity of the band decrease (Figure 9, lanes 10 to 12).

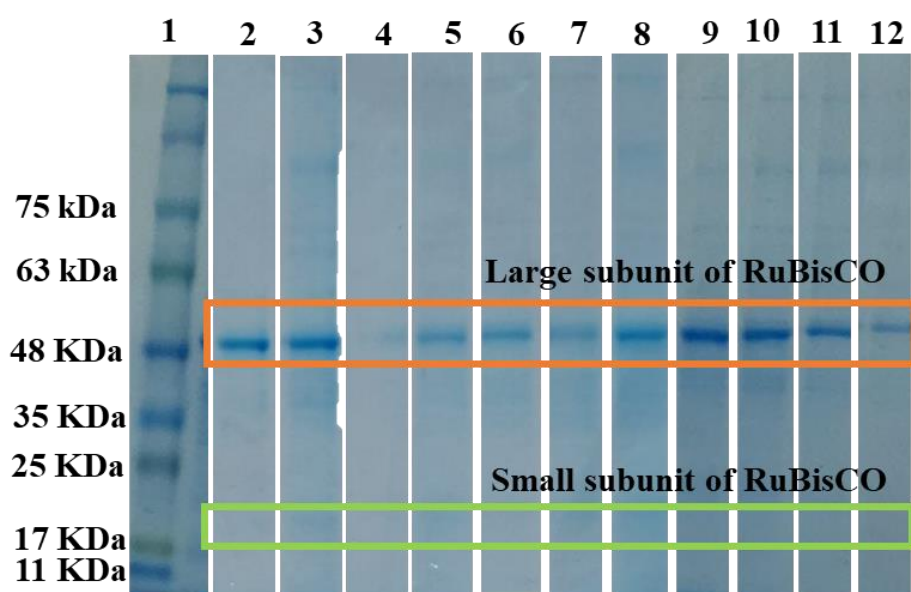


Figure 9. SDS-PAGE stained with BlueSafe. Effect of different aqueous solutions of ILs in the RuBisCO extraction from spinach using the following experimental conditions: IL concentration of 3.3 mM, 0.1 solid-liquid ratio, solid-liquid extraction during 30 min at 29 °C. Lane 1: Standard molecular weights; Lane 2: 1 mg/mL commercial RuBisCO, dissolved in PBS; Lane 3: extract with $[\text{Pr}_3\text{NC}_2\text{OC}_2][\text{Sac}]$; Lane 4: extract with $[\text{Et}_3\text{NC}_2\text{OC}_2][\text{Sac}]$; Lane 5: extract with $[\text{Et}_3\text{NC}_4\text{NC}_4][\text{Br}]$; Lane 6: extract with $[\text{Bu}_3\text{NC}_4\text{NC}_4][\text{Br}]$; Lane 7: extract with $[\text{MpyrNC}_4\text{NC}_4][\text{Br}]$; Lane 8: extract with $[\text{MimNC}_4\text{NC}_4][\text{Br}]$; Lane 9: extract with $[\text{Ch}]\text{Cl}$; Lane 10: extract with $[\text{C}_2\text{mim}]\text{Cl}$; Lane 11: extract with $[\text{C}_4\text{mim}]\text{Cl}$; Lane 12: extract with $[\text{C}_6\text{mim}]\text{Cl}$.

SE-HPLC spectra (Figure 10) demonstrate that $[\text{Ch}]\text{Cl}$ is the only IL capable to extract RuBisCO without the formation of aggregates and, for the others ILs, most of the protein is in the form of aggregates where the peaks from $[\text{MpyrNC}_4\text{NC}_4]\text{Br}$ is the one with a greater area and $[\text{Et}_3\text{NC}_4\text{NC}_4][\text{Br}]$ is the worst IL for RuBisCO extraction. Crossing information with SDS-PAGE, $[\text{MpyrNC}_4\text{NC}_4]\text{Br}$, $[\text{MimNC}_4\text{NC}_4]\text{Br}$, $[\text{Pr}_3\text{NC}_2\text{OC}_2][\text{Sac}]$ and $[\text{Ch}]\text{Cl}$ was tested in other concentrations (from 25 mM to 1M) to check the influence of the concentration in the extraction yield.

Comparing to other proteins, RuBisCO is more susceptible to form aggregates in the presence of ILs due to its dimensions and complexity (composed for several subunits) and due to this fact (14), it is not suspicious that only $[\text{Ch}]\text{Cl}$ were able to extract RuBisCO without some degree of denaturation at low concentration (3.3 mM). As a matter of fact, this response to $[\text{Ch}]\text{Cl}$ in the extraction of proteins was observed by Martins et al. (15) when they chose $[\text{Ch}]\text{Cl}$ because it was able to extract phycobiliproteins at a low concentration and at the same time avoid the extraction of chlorophylls.

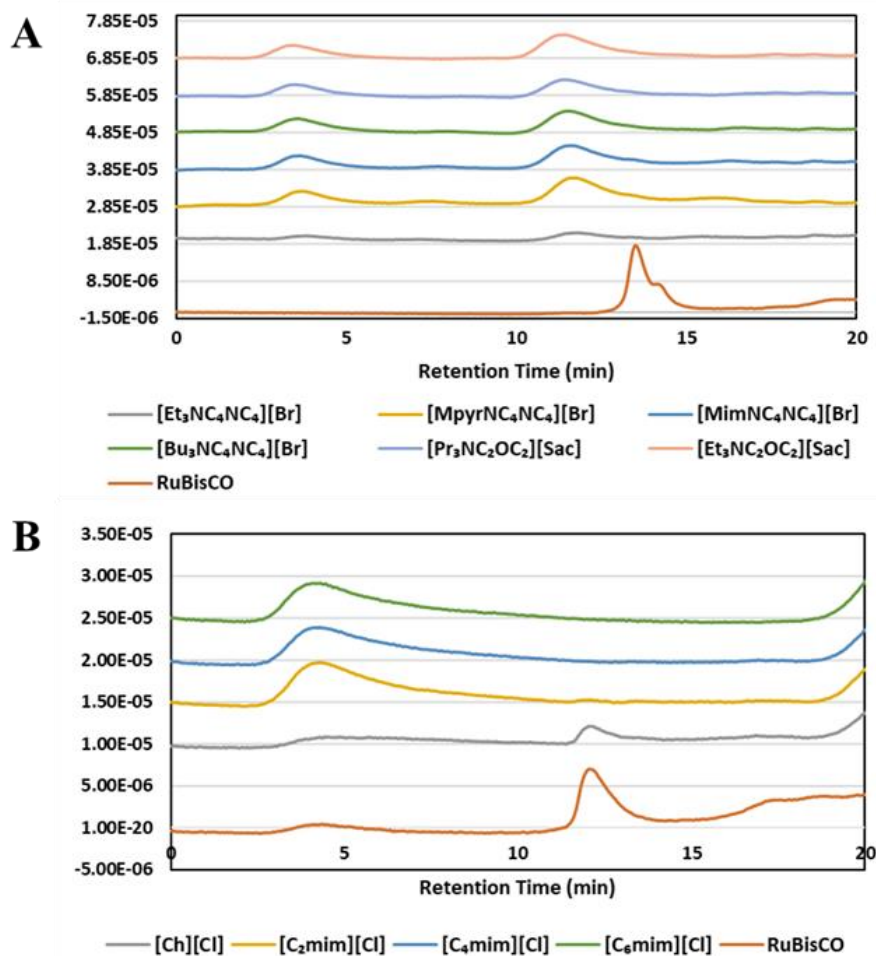


Figure 10. SE-HPLC spectra of aqueous solutions of synthesized ILs (A) and commercial ILs (B) after RuBisCO extraction from spinach leaves with an IL concentration of 3.3 mM.

3.1.2. Effect of ILs concentration on the RuBisCO's extraction

Based on the data previously shown, the most promising ILs in the extraction of RuBisCO were applied in different concentration, 25 mM, 50 mM, 100 mM, 500 mM and 1M, with the exception of [MpyrNC₄NC₄][Br] and [Pr₃NC₂OC₂][Sac] due to their disposable amount in the moment and solubility, respectively, to investigate the effect of ILs concentration in the extraction of RuBisCO. Additionally, [Ch]Br was introduced in this studied to evaluate the effect of bromide anion in the extraction. As in the previous assays, all the experimental conditions were kept constant (600 rpm, a solid-liquid ration of 0.1 and an extraction during 30 min at 29 °C). After the extraction, all extracts were analysed by SDS-PAGE (Figure 12) and SE-HPLC to determine the purity and yield of RuBisCO (Figure 11) according to Equations 3 and 4, respectively.

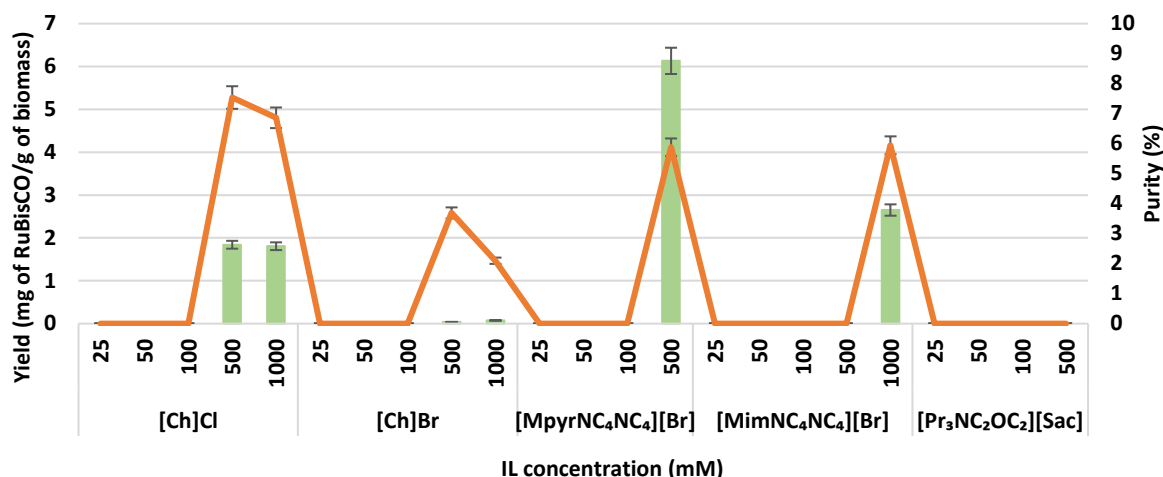


Figure 11. RuBisCO's purity (%), orange line, and yield, green bars, after extraction from spinach leaves using different concentrations of IL (25 mM, 50 mM, 100 mM, 500 mM and 1 M), a solid-liquid ratio of 0.1 in a solid-liquid extraction during 30 min at 29 °C.

Comparing the results of Figures 11 and 12 it is possible to conclude that [Pr₃NC₂OC₂][Sac] didn't extract any protein from spinach, due to the absence of bands in the SDS-PAGE (Figure 12, Gel A, lanes 3-6) and peaks in SE-HPLC chromatograms leading to a RuBisCO yield and purity of zero (Figure 11). Regarding the ILs [MpyrNC₄NC₄]Br and [MimNC₄NC₄]Br (Figure 12, Gel A, lanes 7-15), the presence of the large subunit of RuBisCO is more intense when a higher concentration of IL was applied. These results are in agreement with the analysis by SE-HPLC (Figure 11), where only samples from extraction with aqueous solutions of ILs with higher concentrations (500 mM and 1M) have a yield and purity higher than zero. Contrarily to glycine-betaine-based ILs, [Ch]Cl is the only IL able to extract RuBisCO without denaturation at all concentrations as confirmed by SDS-PAGE (Figure 12, Gel B, lanes 3-7) but with an extraction performance depending on the IL concentration. This is confirmed by yield and purity of RuBisCO determined by SE-HPLC (Figure 11), with samples from extraction with aqueous solutions of ILs with higher concentrations (500 mM and 1M) having a yield and purity higher than zero. Relatively to these two concentrations, at the concentration of IL of 500 mM that a higher yield (6.13 mg of RuBisCO /g of biomass) is achieved with a purity of 5.88 %. This low value of purity, similar to purity values when [MpyrNC₄NC₄]Br 500 mM and [MimNC₄NC₄]Br 1 M were applied is due to other proteins present in the extract and visible in the SDS-PAGE gels (Figure 12). [Ch]Br were used in this investigation to evaluate the effect of bromide anion

in the extraction, however based in Figures 11 and 12 worst results were obtained when compared to [Ch]Cl.

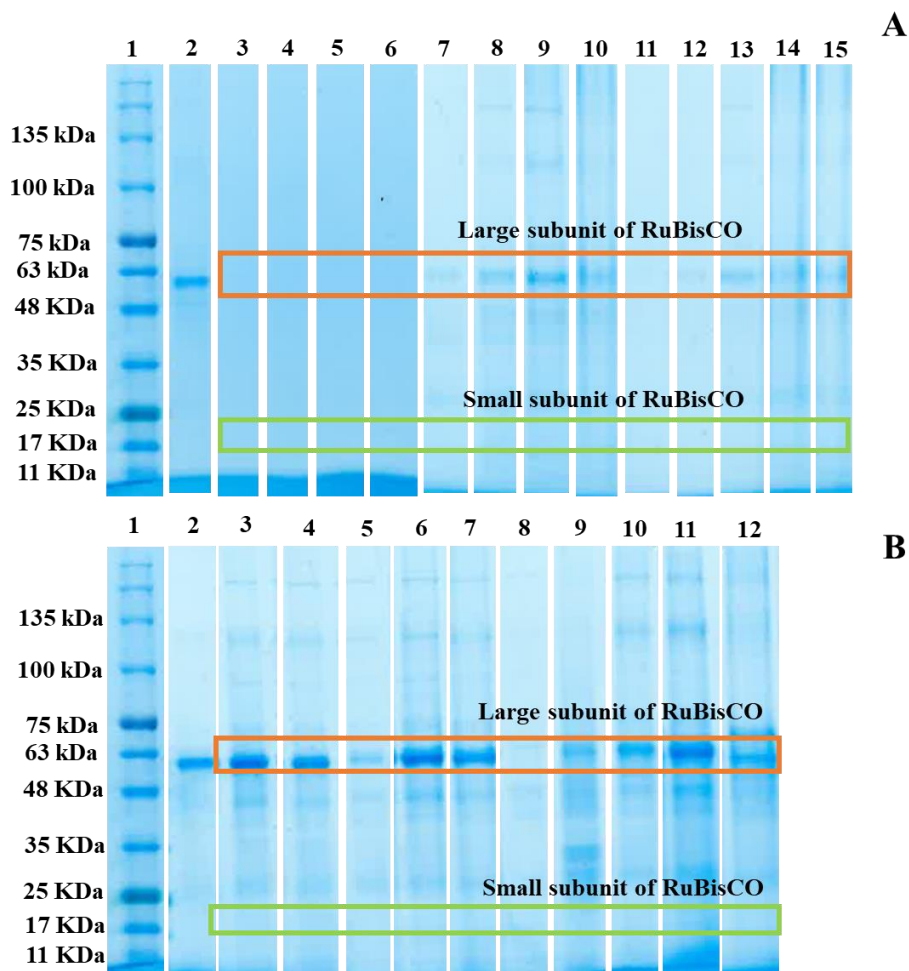


Figure 12. SDS-PAGE stained with BlueSafe. Effect of IL concentration in the RuBisCO extraction from spinach using the following experimental conditions: IL concentration of 25 mM – 1M, 0.1 solid-liquid ratio, solid-liquid extraction during 30 min at 29 °C. **Gel A:** Lane 1: Standard molecular weights; Lane 2: 1 mg/mL commercial RuBisCO, dissolved in PBS; Lanes 3 to 6: extracts with [Pr₃NC₂OC₂][Sac] with the following order of concentrations: 25 mM; 50 mM; 100 mM and 500 mM; Lanes 7 to 10: extracts with [MpyrNC₄NC₄]Br with the following order of concentrations: 25 mM; 50 mM; 100 mM and 500 mM; Lanes 11 to 15: extracts with [MimNC₄NC₄]Br with the following order of concentrations: 25 mM; 50 mM; 100 mM; 500 mM and 1M. **Gel B:** Lane 1: Standard molecular weights; Lane 2: 1 mg/mL commercial RuBisCO, dissolved in PBS; Lanes 3 to 7: extracts with [Ch]Cl with the following order of concentrations: 25 mM; 50 mM; 100 mM; 500 mM and 1 M; Lanes 8 to 12: extracts with [Ch]Br with the following order of concentrations: 25 mM; 50 mM; 100 mM; 500 mM and 1 M.

Taking all these results into account, [Ch]Cl was chosen for RuBisCO extraction and other commercial ILs were tested, for comparison, at the previous concentrations. The reason why [MpyrNC₄NC₄]Br and [MimNC₄NC₄]Br were discarded since they only extracted RuBisCO without aggregation at the highest concentrations (500 mM and 1M), although [MpyrNC₄NC₄]Br was able to extract an unquantifiable concentration of RuBisCO at 100 mM.

Beyond these analyses, the pH value in all the extracts was evaluated. The results show a variation in the pH value between 4.42 and 7.89, with the best results of yield and purity being achieved where, after the SLE, pH value range between 6 and 8. These results are in agreement with the know data about RuBisCO, since between 4.42 and 6 the pH is close to the isoelectric point of the enzyme which is located in the range between 4.6 and 5.5 (depending on the specie), and the best results are located in one of the pH range where the solubility of the enzyme is above 80 % (1,2,18).

3.1.3. Effect of cholinium-based ILs and their concentration on the RuBisCO's extraction

Since [Ch]Cl reveal promising results in the previous assays, other cholinium-based ILs were evaluated in this study, namely [Ch][Acetate], [Ch][DHP] and [Ch][DHC]. Moreover, the IL concentration used in the RuBisCO's extractions were also investigated: 25 mM, 50 mM, 100 mM, 500 mM, and 1 M. The remaining experimental conditions were kept constant (600 rpm, a solid-liquid ratio of 0.1, an extraction during 30 min at 29 °C).

The RuBisCO's purity and yield of extraction were calculated according to Equations 3 and 4, respectively and the results are displayed in Figure 13. SE-HPLC chromatograms from extracts, where [Ch][DHP] and [Ch][DHC] were applied, didn't show any peak, confirming that these ILs are not able to extract RuBisCO. These results were also confirmed by the SDS-PAGE gel (Figure 14) since no bands of protein were detected. Therefore, the results regarding these ILs were not included in Figure 13. Concerning the results obtained with [Ch]Cl and [Ch][Acetate], the last one reveals better RuBisCO's purity ((15.76-57.05)%) and yield of extraction ((2.84-8.45) mg of RuBisCO /g of biomass). These data are in agreement with the SDS-PAGE gel (Figure 14) with a lower number and less intense bands corresponding to other proteins than RuBisCO. The best performance of [Ch][Acetate] can be related to higher protein stability in the presence of this IL. In fact,

[Ch][Acetate] was able to increase the conformational and thermal stability of chymotrypsin with a mild increase in its activity (62).

Relatively to the pH value of extracts, it was observed that the samples from extractions with [Ch][DHP] and [Ch][DHC] have a pH between 3.65 and 5.37, explaining the poor performance of both ILs. As previously reported, the best results are verified when the pH value after extraction is between 6 and 8 since the solubility of the enzyme is above 80 % (1,2).

Selecting [Ch][Acetate] and [Ch]Cl as the best ILs for the extraction of RuBisCO, the next step was the optimization of two parameters: yield of extraction and RuBisCOs' concentration. The purity was not considered since the development of the ABS is to separate and purify the protein in a single step.

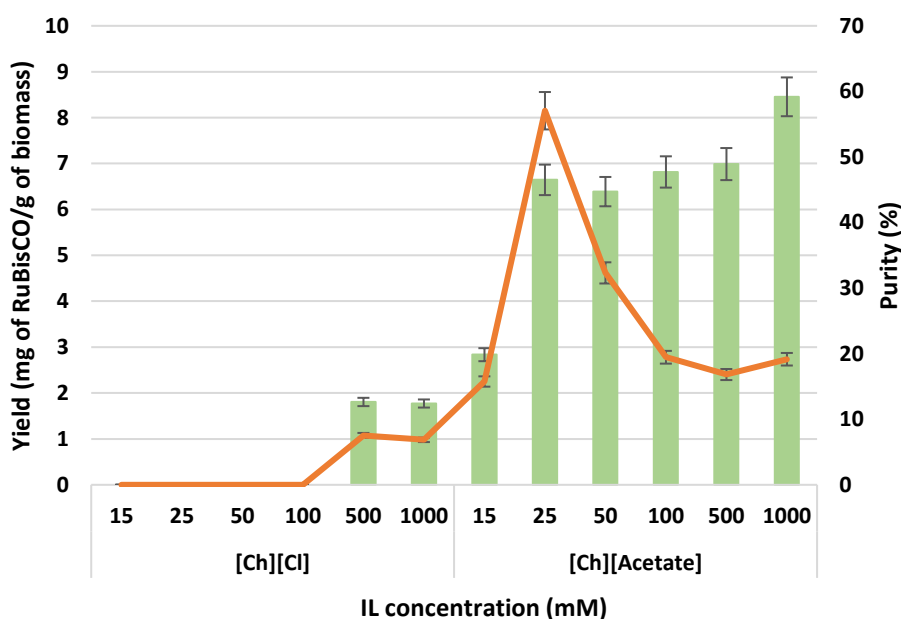


Figure 13. RuBisCO's purity (%), orange line, and yield, green bars, after extraction from spinach leaves using different concentrations of IL (25 mM, 50 mM, 100 mM, 500 mM, and 1 M rpm), a solid-liquid ratio of 0.1 in a solid-liquid extraction during 30 min at 29 °C.

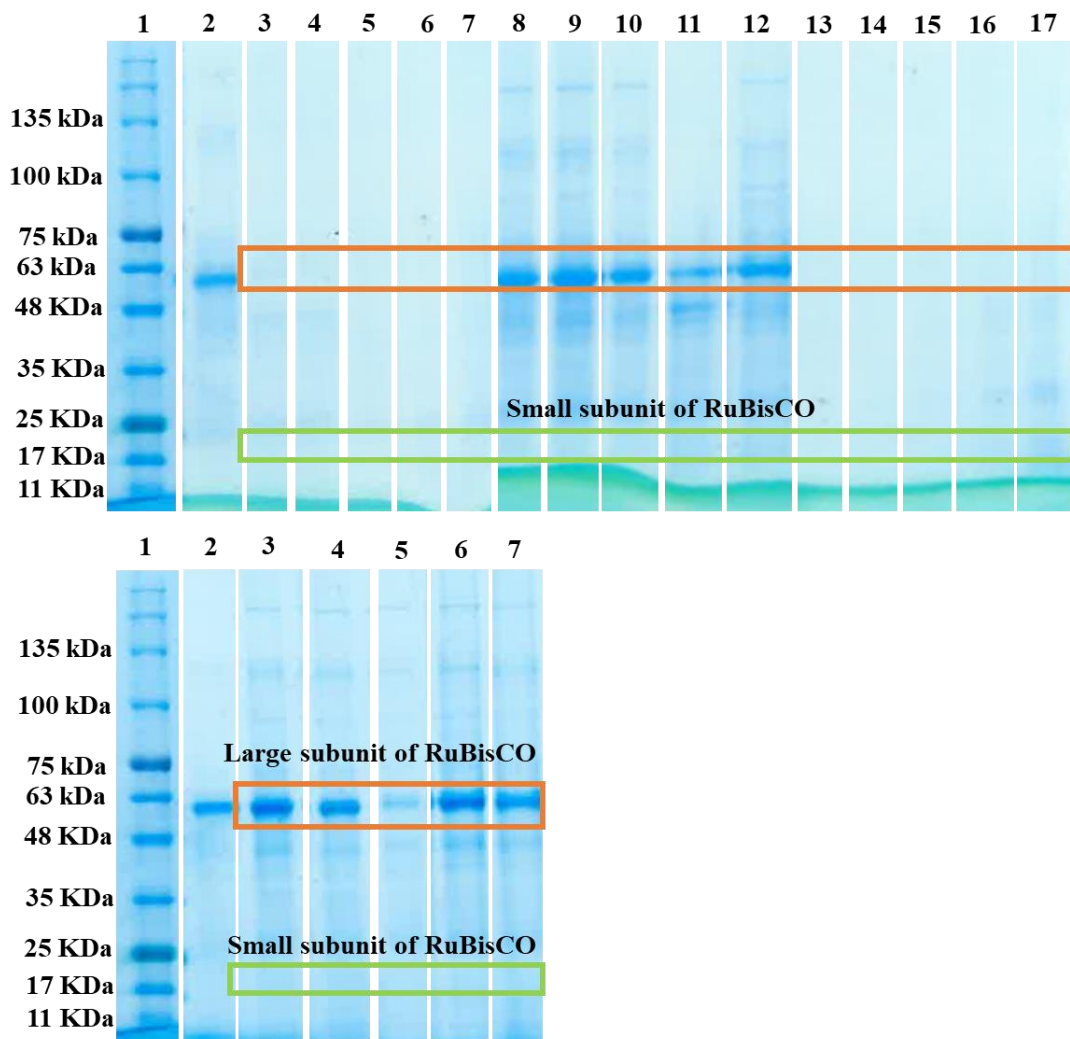


Figure 14. SDS-PAGE stained with BlueSafe. Effect of IL concentration in the RuBisCO extraction from spinach using the following experimental conditions: IL concentration of 25 mM – 1M, 0.1 solid-liquid ratio, solid-liquid extraction during 30 min at 29 °C. **Gel A:** Lane 1: Standard molecular weights; Lane 2: 1 mg/mL commercial RuBisCO, dissolved in PBS; Lanes 3 to 7: extracts with [Ch][DHP] with the following order of concentrations: 25 mM; 50 mM; 100 Mm; 500 mM and 1 M; Lanes 8 to 12 extracts with [Ch][Acetate] with the following order of concentrations: 25 mM; 50 mM; 100 mM; 500 mM and 1 M; Lanes 13 to 17 extracts with [Ch][DHC] with the following order of concentrations: 25 mM; 50 mM; 100 mM; 500 mM and 1 M. **Gel B:** Lane 1: Standard molecular weights; Lane 2: 1 mg/mL commercial RuBisCO, dissolved in PBS; Lanes 3 to 7: extracts with [Ch]Cl with the following order of concentrations: 25 mM; 50 mM; 100 mM; 500 mM and 1 M.

3.2. Response surface methodology (RSM)

The previous extractions allowed the selection of the best ILs but it is necessary to consider the interaction between different factors such as pH, solid-liquid ratio, among others. With the objective to optimize the extraction of RuBisCO and identify the significant conditions, an RSM applying a 2^3 factorial planning was implemented (3 factors and 2 levels). RSM permit the extrapolation of the relationship between the dependent variables (yield of extraction and the concentration of RuBisCO extracted) and the independent variables that can improve the extraction. The factorial planning was performed using [Ch]Cl and [Ch][Acetate] with an extraction time of 30 min, at 29 °C and 600 rpm. The independent variables studied were pH, solid-liquid ratio, and IL concentration.

The results obtained through RSM with the combined effects of solid-liquid ratio and IL concentration, solid-liquid ratio and pH, IL concentration and pH are illustrated in Figures 14-17. The model equation, the experimental conditions, the extraction yield of RuBisCO and the concentration of RuBisCO obtained experimentally and the respective calculated values, as well as the statistical analyses, are provided in Appendix B (Sections B 2 to B 11). Variance analysis (ANOVA) was employed to estimate the statistical significance of the variables and the interactions between them.

3.2.1. Analysis of results for [Ch][Acetate]

For the extractions using [Ch][Acetate], results from the statistical analysis, represented in the pareto chart (Appendix B, Figure B 6.1), show that the significant variables for the yield of extraction are pH and solid-liquid ratio (linear and quadratic). The results of Figure 15 and Appendix B, Table B 4.1 – Figure B 4.1.1 show that pH is the variable with the most significant effect (positive effect in the response) followed by solid-liquid ratio where the linear variable had a positive effect and the quadratic a negative one. The maximum yield of extraction obtained was (10.824 ± 0.485) mg of RuBisCO /g of biomass, for a pH of 11.2, an 0.1 solid-ratio and an IL concentration of 1.5 M. However, above a 0.12 solid-liquid ratio there is a slight decrease in the yield of extraction (Figure 15, (D) and (E)) caused by the effect of the quadratic variable.

Relatively to the concentration of extracted RuBisCO, pareto chart (Appendix B, Figure B 6.2) evidenced that solid-liquid ratio, pH, and their interaction are the significant variables. Taking into account the data represented in Figure 15 and Appendix B, Table B 4.2 – Figure

B 4.2.1, pH is the parameter that has a higher effect on the concentration of extracted RuBisCO and with solid-liquid ratio and their interaction are responsible for the increase of the response. The maximum concentration of extracted RuBisCO obtained was (1.594 ± 0.068) mg/mL, for a pH of 7.0, an 0.184 solid-ratio, and an IL concentration of 1.5 M.

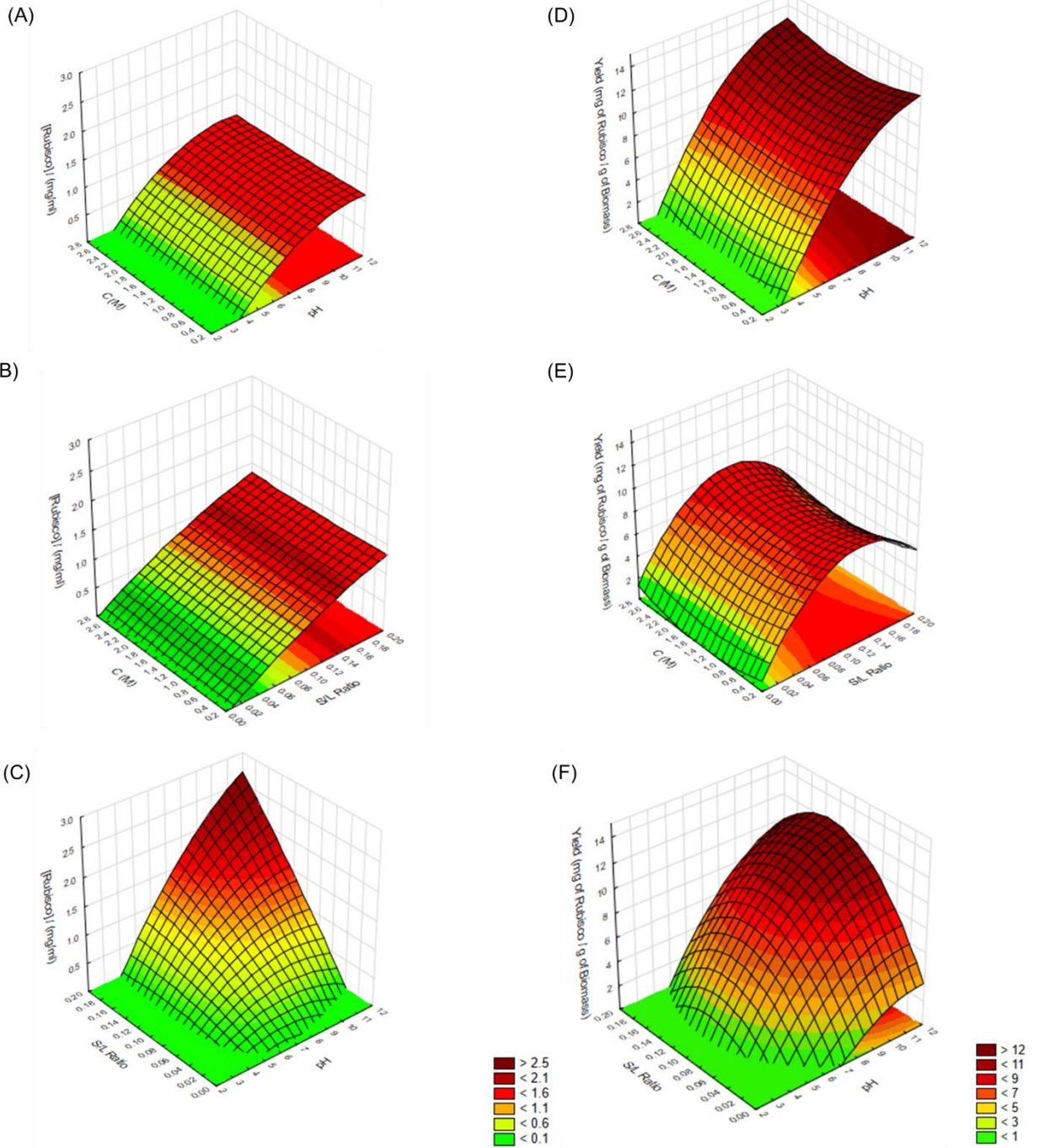


Figure 15. Response surfaces corresponding to the concentration of extracted RuBisCO (left) and yield of extraction (right) with the following combined parameters: (A) and (D) [Ch][Acetate] concentration and pH; (B) and (E) [Ch][Acetate] concentration and solid-liquid ratio; and (C) and (F) solid-liquid ratio and pH.

For both responses, pH is the most significant variable however, other variables affect the responses differently so, it was calculated the best experimental conditions to optimize both responses and were applied in further extractions: a 0.184 solid-liquid ratio, a pH value of 11.2 and an IL concentration of 2.68 M (Appendix B, Figure B 10). The application of a high concentration of IL is this extraction an advantage because in the next step (ABS formation) IL is going to be the salting-out agent and a high concentration facilitates the process. The optimal conditions were tested, and no significant differences were detected between the predicted and observed results, since the concentration of extracted RuBisCO presented only a slight discrepancy between the predicted and the observed value, as shown in Table 2.

Table 2. Results of the extraction with [Ch][Acetate] at the optimal conditions.

	Predicted Results	Observed Results	Relative error (%)
[RuBisCO] (mg/mL)	2.34	2.00	-16.7
Yield (mg of RuBisCO /g of biomass)	11.4	10.9	-3.97

3.2.2. Analysis of results for [Ch]Cl

The statistical results represented in the pareto chart (Appendix B, Figure B 7.1), showed that in the extractions using [Ch]Cl as a solvent, the solid-liquid ratio and IL concentration are the significant parameters on the yield of extraction. The results of Figure 16 and in Appendix B, Table B 5.1 – Figure B 5.1.1, showed that the solid-liquid ratio has a negative effect and pH and [Ch]Cl concentration have a positive effect on the response. The maximum yield of extraction obtained was (14.05 ± 0.69) mg of RuBisCO /g of biomass, for a pH of 7.0, an 0.016 solid-ratio, and an IL concentration of 1.5 M.

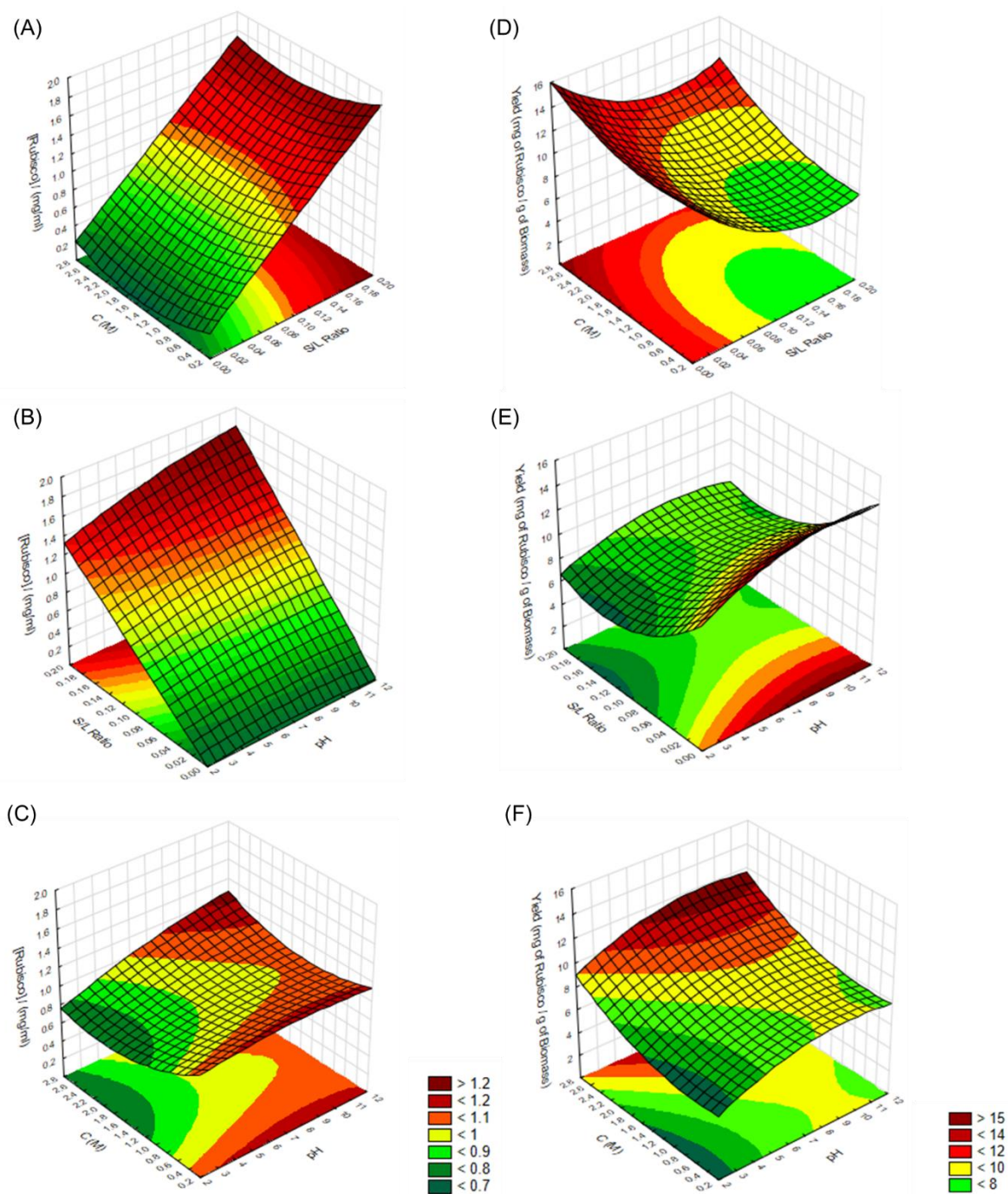


Figure 16. Response surfaces corresponding to the concentration of extracted RuBisCO (left) and yield of extraction (right) with the following combined parameters: (A) and (D) [Ch]Cl concentration and solid-liquid ratio; (B) and (E) solid-liquid ratio and pH; and (C) and (F) [Ch]Cl concentration and pH.

For the concentration of extracted RuBisCO, the pareto chart (Appendix B, Figure B 7.2) evidenced that the solid-liquid ratio and pH are the significant variables. Taking into account the data represented in Figure 16 and Appendix B, Table B 5.2 – Figure B 5.2.1, the solid-liquid ratio is the parameter that has a higher effect on the concentration of extracted RuBisCO with a positive effect on the response, and pH and the concentration of [Ch]Cl (quadratic) did not affect in a significant way the increase of the response. The maximum concentration of extracted RuBisCO obtained was (1.37 ± 0.07) mg/mL, for a pH of 9.5, an 0.15 solid-ratio and an IL concentration of 0.80 M.

Since each response is affected by different variables, the best experimental conditions, to increase both responses, were calculated and applied in further extractions: a 0.184 solid-liquid ratio, a pH value of 9.09 and an IL concentration of 2.68 M (Appendix B, Figure B 11). As said before, also here the application of a high concentration of IL is this extraction an advantage because in the next step (ABS formation) IL is going to be the salting-out agent and a high concentration facilitates the process. The optimal conditions were tested, and no significant differences were detected between the predicted and observed results, as shown in Table 3.

Table 3. Results of the extraction with [Ch]Cl at the optimal conditions.

	Predicted Results	Observed Results	Relative error (%)
[RuBisCO] (mg/mL)	1.72	1.86	7.51
Yield (mg of RuBisCO /g of biomass)	11.6	10.1	-14.1

In order to compare the performance of ILs in the extraction of RuBisCO from spinach with the solvent commonly used, the NH₄OH (3) was also evaluated. An aqueous solution of NH₄OH 0.1M at pH 11 was applied in the RuBisCO's extraction from spinach, and the remaining extraction conditions were maintained (600 rpm, a solid-liquid ratio of 0.1, during

30 min, at 29 °C). The results obtained and the comparison with [Ch]Cl and [Ch][Acetate] are demonstrated in Figures 17 and 18.

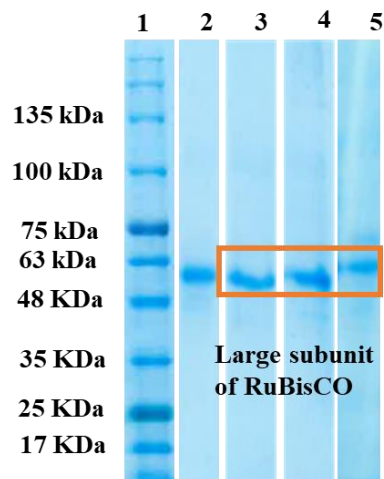


Figure 17. SDS-PAGE stained with BlueSafe. Lane 1: Standard molecular weights; Lane 2: 1 mg/mL commercial RuBisCO, dissolved in PBS; Lane 3: spinach extracts with [Ch][Acetate]; Lane 4: spinach extracts with [Ch]Cl; Lane 5: spinach extract with NH_4OH .

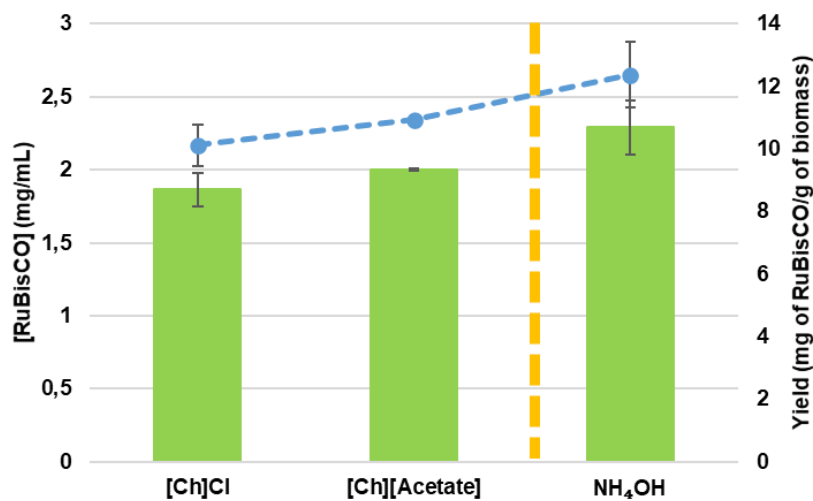


Figure 18. RuBisCO's yield, blue stroke, and RuBisCO's concentration, green bars, after extraction from spinach leaves at the optimal conditions and with NH_4OH , a solid-liquid ratio of 0.1 in a solid-liquid extraction during 30 min at 29 °C.

The application of NH_4OH for RuBisCO extraction reveals results slightly better than the ones obtained with aqueous solutions of ILs, since higher concentration of RuBisCO

(2.29 mg/mL *versus* 2.00 mg/mL and 1.86 mg/mL) and extraction yield (12.38 mg of RuBisCO /g of biomass *versus* 10.12 mg of RuBisCO /g of biomass and 10.93 mg of RuBisCO /g of biomass) were obtained with the conventional solvent, using the same conditions of extraction. However, it should keep in mind that other variables must be evaluated, such as protein stability, if it is possible to integrate with another process/technique. Furthermore, cholinium-based ILs were developed as possible substitutes to others with toxicity problems that put in cause the biocompatibility and biodegradability of the systems (14,32).

3.3. RuBisCOs' purification with ABS

Considering that the extracts previously obtained in the SLE, specifically with the most promising ILs ([Ch]Cl and [Ch][Acetate]), are complex and contain several biomolecules, a purification step is required in order to obtain a higher pure sample of RuBisCO. In this sense, ABS was applied to separate RuBisCO from one of the aqueous phases while the remaining proteins are expected to migrate to the opposite phase. However, cholinium-based ILs tend to be highly hydrophilic and only form ABS with strong salting-out salts (*e.g.*, K_3PO_4 and K_2CO_3) or with polymers (*e.g.*, PPG 400 and 1000, PEG 400, 600 and 1000), in which the IL may act as the salting-out species (63). Therefore, in this work PPG 400, PEG 1000 were selected as the second compound of the ABS due to strong evidence that proteins are stable in the presence of certain polymers (14). The mixture compositions of the ABS were selected based on the report of Pereira et al. (59). Using PPG 400, the mixture point 15 wt% of [Ch][Acetate] + 19 wt% of water + 67 wt% of polymer and 12 wt% of [Ch]Cl + 21 wt% of water + 67 wt% of polymer were chosen while for PEG 1000 the biphasic mixture 15 wt% of [Ch][Acetate] + 19 wt% of water + 67 wt% of polymer and 12 wt% of [Ch]Cl + 21 wt% of water + 67 wt% of polymer were selected. For all the systems, the weight percentage of IL and water derived from the extracts. Briefly, after extraction with each IL, it was added to an aliquot of 1 g of extract 2 g of each polymer. The obtained ABSs are showed in Figure 19 and as depicted in Figure 19, the top phase (polymer-rich phase) of the ABS composed of PEG 1000 has a very small phase. Consequently, only PPG 400 was selected for the RuBisCOs' purification. Additionally, in this ABS the formation of a precipitate in the interphase that extends to the top phase was observed (Figure 19). This precipitated may be RuBisCO or other biomolecules present in the spinach extract. To clarify

and verify if the RuBisCO purification was succeeded both phases and interphase precipitated were analysed by SDS-PAGE and SE-HPLC.

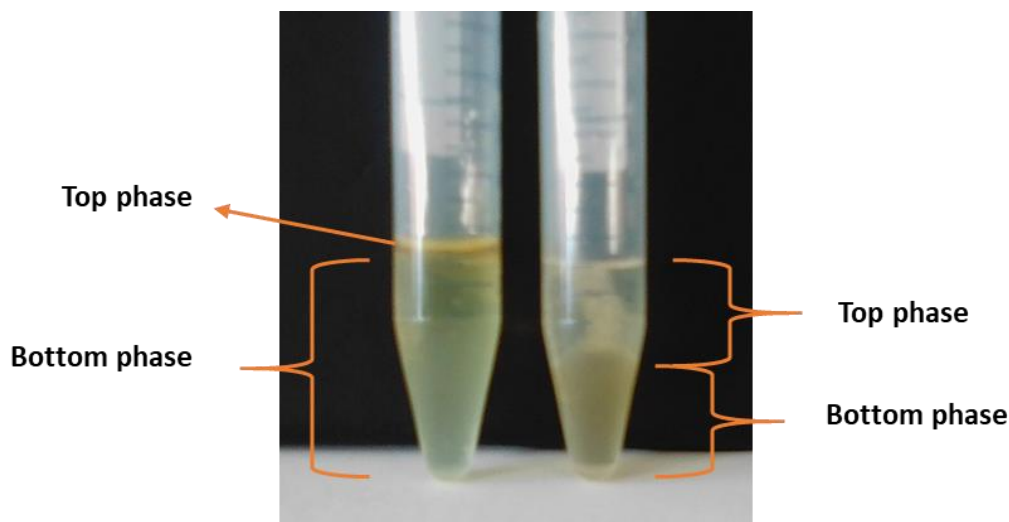


Figure 19. ABS composed by PEG 1000+ spinach extract with [Ch][Acetate] (left) and PPG 400 + spinach extract with [Ch][Acetate] (right).

Only with the ABS composed of PPG 400 + [Ch][Acetate] the presence of RuBisCO in the bottom-phase (IL-rich phase) is noticed in the protein profile analysed through SDS-PAGE. This result agrees with the SE-HPLC analysis (Figure 20) since only in the chromatograms of the bottom phase of this ABS the presence of different peaks, including the peak corresponding to RuBisCO, appear. With ABS composed of PPG 400 + [Ch][Acetate] an extraction efficiency ($EE\%$) of RuBisCO of 100% was obtained and a recovery of (1.34 ± 0.36) mg of RuBisCO of the initials (1.36 ± 0.006) mg of RuBisCO, meaning a yield of 100%. Although a good yield was obtained, a lower value of purity was attained ($(22.67 \pm 2.06)\%$). Despite the absence of other bands in SDS-PAGE, the SE-HPLC spectra show a great amount of protein eluted between the 15 and 20 min, decreasing the purity of the protein. Taken the purity into account it is evidenced that this ABS is not selective for RuBisCO and consequently is not adequate for its purification. There are some studies about RuBisCO partitioning in ABS with polymer and ILs. Preferably, the polymer used is PEG due its capability of stabilize the proteins and, in fact in the examples with RuBisCO when PEG was present in the ABS, RuBisCO partitioned in majority for the PEG-rich phase. In this work the selected compounds were PPG 400 and cholinium-based ILs in which the used ILs are well-known for their biocompatibility, biodegradability, low toxicity,

and the capability to stabilize the target protein. So, it was expected that on PPG 400 + cholinium-based ILs studied in this work, RuBisCO partitioned in its majority for the IL-rich phase (bottom phase) (11,14,32,64).

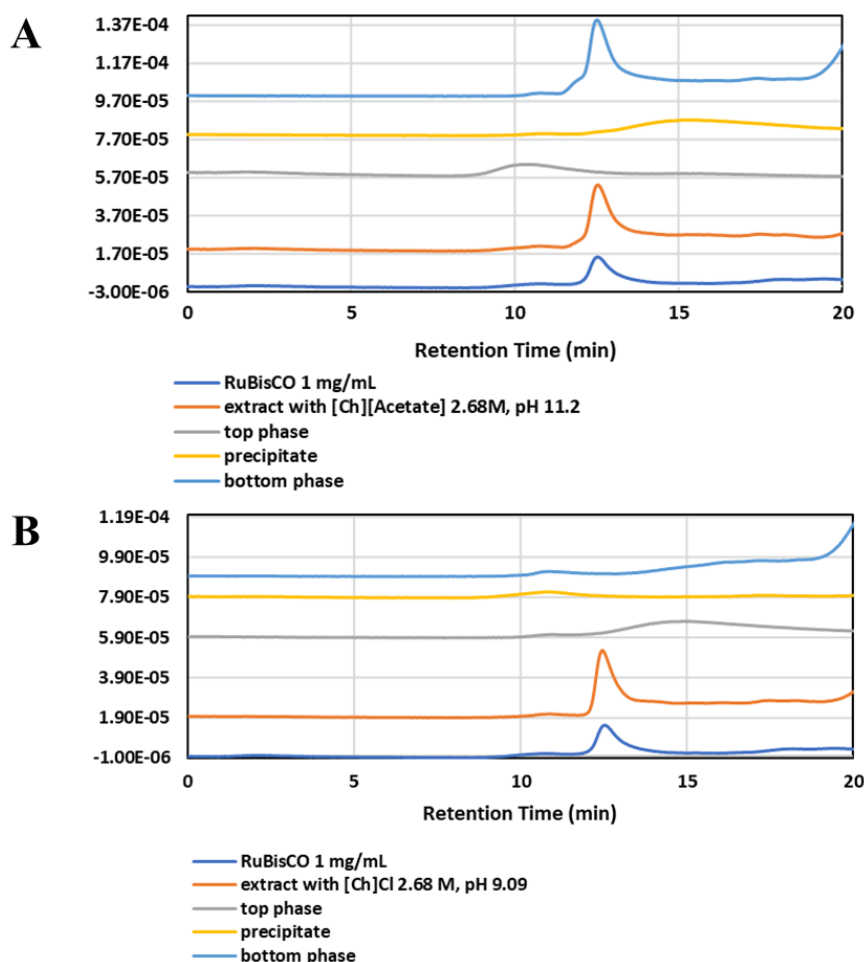


Figure 20. SE-HPLC spectra of the different extracts, phases, and precipitates of the ABSs composed by IL and PPG 400, where (A) is for [Ch][Acetate] and (B) for [Ch]Cl.

Since the ABS with PPG 400 is not selective for RuBisCO, a ternary mixture composed by the extract (contributor for the water and IL weight percentages) and K_2HPO_4 . The selected ternary mixtures 27 wt% of [Ch][Acetate] + 44 wt% of water + 29 wt% of K_2HPO_4 and 24 wt% of [Ch]Cl + 48 wt% of water + 29 wt% of K_2HPO_4 determined by Belchior *et al.* (60) and Osloob *et al.* (61) respectively. As in the previous ABSs, after the extractions with each IL, it was added to an aliquot of 1 g of extract 0.6 g of K_2HPO_4 . After the phases' separation the ABS showed in Figure 21 were obtained and each phase was analysed by SDS-PAGE and SE-HPLC.

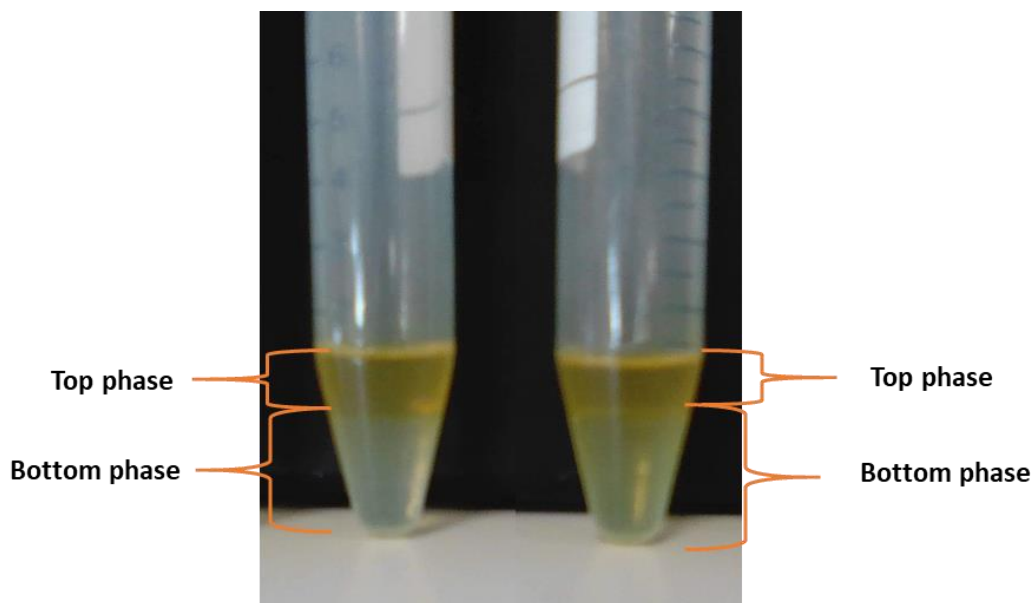


Figure 21. ABS composed by K_2HPO_4 + spinach extract with [Ch][Acetate] (left) and K_2HPO_4 + spinach extract with [Ch]Cl (right).

In both ABSs, by the analysis of the protein profile in SDS-PAGE, RuBisCO partitioned to the top phase (IL-rich phase) and for the precipitate. This result agrees with the SE-HPLC analysis, Figure 22, since only in the chromatograms of the top phase and precipitate the presence of different peaks, including the peak corresponding to RuBisCO appears although in unquantifiable amounts in the precipitate. With these ABSs, extraction efficiencies ($EE\%$) for RuBisCO of 100% were obtained and the K confirm the complete extraction of RuBisCO. Relatively to the extraction yield, for the system with [Ch][Acetate] it was possible to recover (0.72 ± 0.09) mg of RuBisCO of the initials (1.43 ± 0.097) mg of RuBisCO, meaning a yield of $(50.4 \pm 9.96)\%$ and, for the system with [Ch]Cl it was possible to recover (0.77 ± 0.30) mg of RuBisCO of the initials (1.55 ± 0.389) mg of RuBisCO, meaning a yield of $(54.5 \pm 0.639)\%$. These results show that the ABSs composed of PPG 400 had the best yield of extraction, but in terms of purity ($(35.1 \pm 1.40)\%$ for [Ch][Acetate] and $(12.9 \pm 0.668)\%$ for [Ch]Cl) both ABSs with salt and polymer are not selective for RuBisCO. The results are in agreement with the conclusions of several publications like the work from Belchior *et al.* (60) that were able to extract several amino acids with the ABS composed by [Ch][Acetate] + K_2HPO_4 . They obtained extraction efficiencies above 95% although they only achieve a complete extraction for L-tryptophan. The ABS composed of

[Ch]Cl and K_2HPO_4 was studied by Osloob *et al.* (61) for the partition of penicillin G and 96 % of the biomolecule partition to the IL-rich phase. Relatively to RuBisCO, Desai *et al.* (11) report the RuBisCO migration to IL-rich phase in an ABS composed by Iolilyte 221PG and sodium potassium buffer and Ruiz *et al.* (14) observe the same behavior for the ABS with Iolilyte 221PG and potassium buffer. For biological matrices, an ABS with K_2HPO_4 and 1-butyl-3-methylimidazolium chloride was studied to extract the proteins of human urine by Du *et al.* (65), where it was observed that all the proteins partitioned to the top phase (IL-rich) and the metal species migrated to the salt-rich phase.

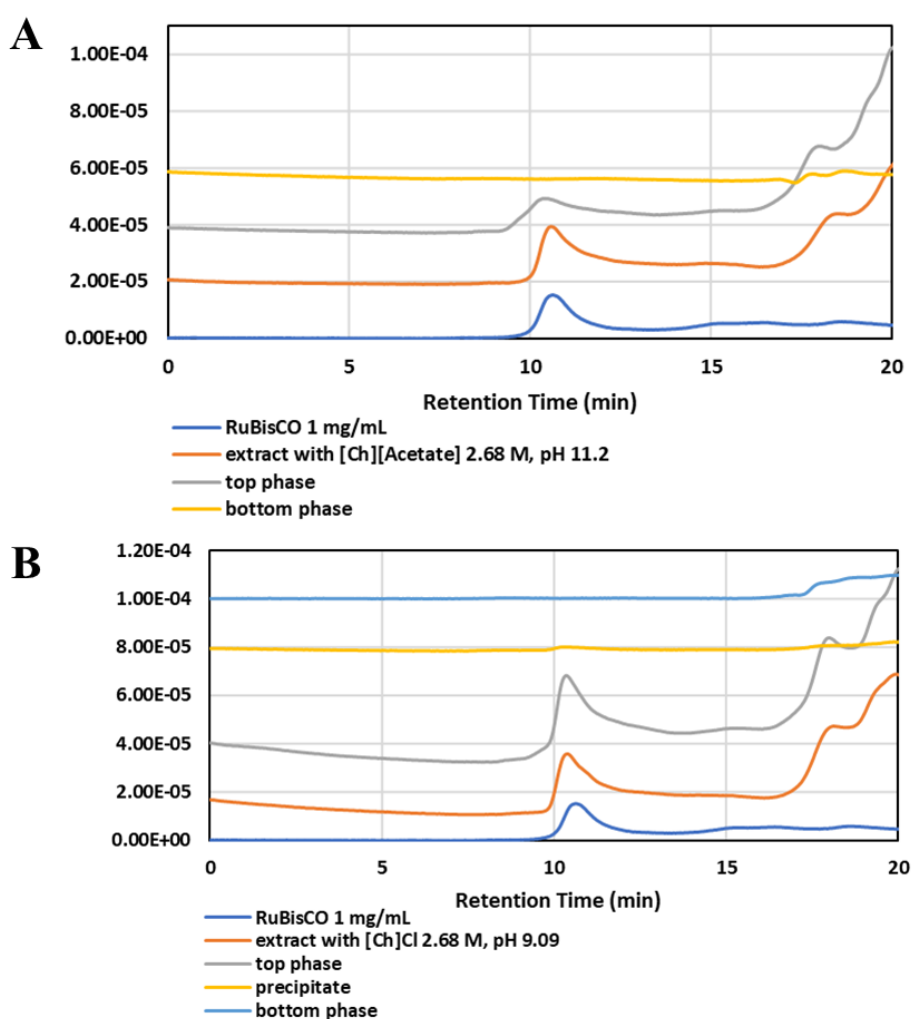


Figure 22. SE-HPLC spectra of the different extracts, phases, and precipitates of the ABSs composed by IL and K_2HPO_4 , where (A) is for [Ch][Acetate] and (B) for [Ch]Cl.

4. Final Remarks

Conclusions

In this work it was developed a new SLE method for RuBisCO from spinach with aqueous solutions of ILs with the aiming of integrating the extract in a separation/purification step through the formation of an ABS. An initial screening, where the effect of ILs in the extraction of RuBisCO from spinach was evaluated showed that $[\text{Et}_3\text{NC}_4\text{NC}_4][\text{Br}]$ and $[\text{Et}_3\text{NC}_2\text{OC}_2][\text{Sac}]$ are the worst ILs to extract RuBisCO and, that $[\text{MpyrNC}_4\text{NC}_4]\text{Br}$, $[\text{MimNC}_4\text{NC}_4]\text{Br}$, $[\text{Pr}_3\text{NC}_2\text{OC}_2][\text{Sac}]$, $[\text{Ch}]\text{Cl}$ and $[\text{C}_2\text{mim}]\text{Cl}$ were the most promising ILs. However, the extractions using $[\text{C}_2\text{mim}]\text{Cl}$, $[\text{C}_4\text{mim}]\text{Cl}$ and $[\text{C}_6\text{mim}]\text{Cl}$ were affected by the length of the carbon chain, where the increase of the carbon chain length decreased the extraction yield. In fact, $[\text{Ch}]\text{Cl}$ was the only IL able to extract RuBisCO without the formation of aggregates. A new screening with variation of IL concentration was made and $[\text{Ch}]\text{Cl}$ was the only one able to extract RuBisCO without denaturation at all concentrations. The study of other cholinium-based ILs bring to this work $[\text{Ch}][\text{Acetate}]$.

The extractions were optimized through a RSM and the optimal conditions were: a 0.184 solid-liquid ratio, an IL concentration of 2.68 M and a pH of 9.09 for $[\text{Ch}]\text{Cl}$ and a pH of 11.2 for $[\text{Ch}][\text{Acetate}]$. These results were verified and validated for both ILs and comparing with an extraction where the solvent of the conventional method was applied, the results are similar although the results with the conventional solvent are slightly better. However, it is necessary to evaluate the further steps for separation and purification in the choice of the best solvent.

To separate and purify RuBisCO from the other proteins and contaminants, it was studied two ABSs composed by IL + water + PPG 400 and IL + water + K_2HPO_4 . For the ABS with PPG 400, the one with $[\text{Ch}][\text{Acetate}]$ was the only one to achieve the goal without the degradation of the target biomolecule with an EE% of 100% since RuBisCO partitioned in totality for the bottom phase; the same happened in the ABS with K_2HPO_4 with the exception that both ABS (with $[\text{Ch}][\text{Acetate}]$ and $[\text{Ch}]\text{Cl}$) achieve the goal and the protein partitioned to the top phase. Nevertheless, these ABSs are not selective for RuBisCO for the reason that in ABSs with PPG 400 all the phases have protein (in the bottom phase there are others in addition to RuBisCO) and in K_2HPO_4 case, all the protein migrates to the top-phase and due to this they cannot be applied in the purification of RuBisCO.

Future work

In this work, it was developed a new SLE method for RuBisCO from spinach leaves with aqueous solutions of ILs with the intention of integrating with a separation/purification step through the formation of an ABS. Numerous ILs were studied and the best were selected. The extraction was optimized, and it was created an ABS with the addition of a polymer or a salt to the extract. Even though RuBisCO partition in totality for one of the phases it is necessary further investigations to find a better ABS since these are not selective.

Based on the results, the next step should be focused on the improvement of the ABS selectivity. After that, it can be interesting to investigate if it is possible to do consecutive extractions until the IL solution is saturated with RuBisCO and applied the ABS in the end. Another possibility related to the sustainability of the process that can be investigated is if it is possible to recycle the phases of the ABS. Of course, that all of these improvements in the method have to consider the stability and activity of the target protein.

5. References

1. Martin AH, Castellani O, De Jong GAH, Bovetto L, Schmitt C. Comparison of the functional properties of RuBisCO protein isolate extracted from sugar beet leaves with commercial whey protein and soy protein isolates. *J Sci Food Agric.* 2019;99:1568–76.
2. Di Stefano E, Agyei D, Njoku EN, Udenigwe CC. Plant RuBisCo: An Underutilized Protein for Food Applications. *JAOCs, J Am Oil Chem Soc.* 2018;95(8):1063–74.
3. Kobbi S, Bougatef A, Le flem G, Balti R, Mickael C, Fertin B, et al. Purification and Recovery of RuBisCO Protein from Alfalfa Green Juice: Antioxidative Properties of Generated Protein Hydrolysate. *Waste and Biomass Valorization.* 2017;8:493–504.
4. Tenorio AT, Kyriakopoulou KE, Suarez-Garcia E, van den Berg C, van der Goot AJ. Understanding differences in protein fractionation from conventional crops, and herbaceous and aquatic biomass - Consequences for industrial use. *Trends Food Sci Technol.* 2018;71:235–45.
5. Dotsenko G, Lange L. Enzyme Enhanced Protein Recovery from Green Biomass Pulp. *Waste and Biomass Valorization.* 2017;8:1257–64.
6. Tenorio AT, Gieteling J, De Jong GAH, Boom RM, Van Der Goot AJ. Recovery of protein from green leaves: Overview of crucial steps for utilisation. *Food Chem.* 2016;203:402–8.
7. Zhang C, Sanders JPM, Bruins ME. Critical parameters in cost-effective alkaline extraction for high protein yield from leaves. *Biomass and Bioenergy.* 2014;67:466–72.
8. Bracher A, Whitney SM, Hartl FU, Hayer-Hartl M. Biogenesis and Metabolic Maintenance of Rubisco. *Annu Rev Plant Biol.* 2017;68:29–60.
9. Hanson DT. Breaking the rules of Rubisco catalysis. *J Exp Bot.* 2016;67:3180–2.
10. Orr DJ, Carmo-Silva E. Extraction of RuBisCO to determine catalytic constants. Covshoff S, editor. Vol. 1770, *Photosynthesis: Methods and Protocols, Methods in Molecular Biology.* Humana Press, New York, NY; 2018. 229–238 p.
11. Desai RK, Streefland M, Wijffels RH, Eppink MHM. Extraction and stability of selected proteins in ionic liquid based aqueous two phase systems. *Green Chem.* 2014;16:2670–9.
12. D'Alvise N, Lesueur-Lambert C, Fertin B, Dhulster P, Guillochon D. Removal of polyphenols and recovery of proteins from alfalfa white protein concentrate by

- ultrafiltration and adsorbent resin separations. *Sep Sci Technol*. 2000;35(15):2453–72.
13. Libouga DG, Aguié-Béghin V, Douillard R. Thermal denaturation and gelation of rubisco: Effects of pH and ions. *Int J Biol Macromol*. 1996;19(4):271–7.
 14. Suarez Ruiz CA, van den Berg C, Wijffels RH, Eppink MHM. Rubisco separation using biocompatible aqueous two-phase systems. *Sep Purif Technol*. 2018;196:254–61.
 15. Martins M et al., Vieira FA, Correia I, Ferreira RAS, Abreu H, Coutinho JAP, et al. Recovery of phycobiliproteins from the red macroalga *Gracilaria* sp. using ionic liquid aqueous solutions. *Green Chem*. 2016;18(15):4287–96.
 16. Tcherkez GGB, Bathellier C, Stuart-Williams H, Whitney S, Gout E, Bligny R, et al. D₂O solvent isotope effects suggest uniform energy barriers in ribulose-1,5-bisphosphate carboxylase/oxygenase catalysis. *Biochemistry*. 2013;52(5):869–77.
 17. Tabita FR, Satagopan S, Hanson TE, Kreel NE, Scott SS. Distinct form I, II, III, and IV Rubisco proteins from the three kingdoms of life provide clues about Rubisco evolution and structure/function relationships. *J Exp Bot*. 2008;59(7):1515–24.
 18. Martin AH, Nieuwland M, De Jong GAH. Characterization of heat-set gels from RuBisCO in comparison to those from other proteins. *J Agric Food Chem*. 2014;62(44):10783–91.
 19. Cummins PL, Kannappan B, Gready JE. Ab Initio Molecular Dynamics Simulation and Energetics of the Ribulose-1,5-biphosphate Carboxylation Reaction Catalyzed by Rubisco: Toward Elucidating the Stereospecific Protonation Mechanism. *J Phys Chem B*. 2019;123(12):2679–86.
 20. Bagheri R, Ahmad J, Bashir H, Iqbal M, Qureshi MI. Changes in rubisco, cysteine-rich proteins and antioxidant system of spinach (*Spinacia oleracea* L.) due to sulphur deficiency, cadmium stress and their combination. *Protoplasma*. 2017;254(2):1031–43.
 21. Lin Z-H, Zhong Q-S, Chen C-S, Ruan Q-C, Chen Z-H, You X-M. Carbon dioxide assimilation and photosynthetic electron transport of tea leaves under nitrogen deficiency. *Bot Stud*. 2016;57(37).
 22. McNevin D, Von Caemmerer S, Farquhar G. Determining RuBisCO activation kinetics and other rate and equilibrium constants by simultaneous multiple non-linear

- regression of a kinetic model. *J Exp Bot.* 2006;57(14):3883–900.
23. Keown JR, Pearce FG. Characterization of spinach ribulose-1,5-bisphosphate carboxylase/oxygenase activase isoforms reveals hexameric assemblies with increased thermal stability. *Biochem J.* 2014;464(3):413–23.
 24. Zhu Y, Huang Z, Chen Q, Wu Q, Huang X, So PK, et al. Continuous artificial synthesis of glucose precursor using enzyme-immobilized microfluidic reactors. *Nat Commun.* 2019;10(4049).
 25. Kaufmann B, Christen P. Recent extraction techniques for natural products: Microwave-assisted extraction and pressurised solvent extraction. *Phytochem Anal.* 2002;13(2):105–13.
 26. Dolashka-Angelova P, Ali SA, Demirevska-Kepova K, Stoeva S, Voelter W. Purification, characterization and thermostability of ribulose 1,5-bisphosphate carboxylase-oxygenase from barley leaves. *Zeitschrift fur Naturforsch - Sect C J Biosci.* 2000;55:611–9.
 27. Gamse T. Extraction-High Pressure Extraction. *Dep Chem Eng Environ Technol.* 1998;1–37.
 28. Walter H, Brooks DE, Fisher D. *Partitioning in Aqueous Two-Phase Systems: Theory, Methods, Uses, and Applications to Biotechnology.* 2nd ed. London Academic Press. 1985.
 29. Ferreira AM, Freire MG. Extração e Purificação de Produtos de Valor Acrescentado Utilizando Sistemas Aquosos Bifásicos Constituídos por Líquidos Iônicos. *Soc Port Quim.* 2015;139:23–34.
 30. Graenacher C. *Cellulose Solution.* United States of America: Graenacher, Charles; 1931.
 31. Divya MB, Guruprasad L. Activity and thermal stability of Mycobacterium tuberculosis PE1 and PE2 proteins esterase domain in the presence of aprotic ionic liquids. *Spectrochim Acta - Part A Mol Biomol Spectrosc.* 2020;225:117477–86.
 32. Sahoo DK, Jena S, Tulsian KD, Dutta J, Chakrabarty S, Biswal HS. Amino-Acid-Based Ionic Liquids for the Improvement in Stability and Activity of Cytochrome c: A Combined Experimental and Molecular Dynamics Study. *J Phys Chem B.* 2019;123:10100–9.
 33. Cláudio AFM, Ferreira AM, Freire MG, Coutinho JAP. Enhanced extraction of

- caffeine from guaraná seeds using aqueous solutions of ionic liquids. *Green Chem.* 2013;15(7):2002–10.
34. Martins M, Fernandes APM, Torres-Acosta MA, Collén PN, Abreu MH, Ventura SPM. Extraction of chlorophyll from wild and farmed *Ulva* spp. using aqueous solutions of ionic liquids. *Sep Purif Technol.* 2021;254:117589–96.
 35. Martínez-Aragón M, Burghoff S, Goetheer EL V., de Haan AB. Guidelines for solvent selection for carrier mediated extraction of proteins. *Sep Purif Technol.* 2009;65:65–72.
 36. Albertsson PÅA. Partition of proteins in liquid polymer-polymer two-phase systems. *Nature.* 1958;182:709–11.
 37. Song CP, Yap QY, Chong MYA, Ramakrishnan Nagasundara R, Vijayaraghavan R, Macfarlane DR, et al. Environmentally Benign and Recyclable Aqueous Two-Phase System Composed of Distillable CO₂-Based Alkyl Carbamate Ionic Liquids. *ACS Sustain Chem Eng.* 2018;6(8):10344–54.
 38. Ruiz CAS, Emmery DP, Wijffels RH, Eppink MHM, van den Berg C. Selective and mild fractionation of microalgal proteins and pigments using aqueous two-phase systems. *J Chem Technol Biotechnol.* 2018;93(9):2774–83.
 39. Silvério SC, Rodríguez O, Tavares APM, Teixeira JA, Macedo EA. Laccase recovery with aqueous two-phase systems: Enzyme partitioning and stability. *J Mol Catal B Enzym.* 2013;87:37–43.
 40. González-Tello P, Camacho F, Blázquez G, Alarcón FJ. Liquid-liquid equilibrium in the system poly(ethylene glycol) + MgSO₄ + H₂O at 298 K. *J Chem Eng Data.* 1996;41(6):1333–6.
 41. Pei Y, Li Z, Liu L, Wang J, Wang H. Selective separation of protein and saccharides by ionic liquids aqueous two-phase systems. *Sci China Chem.* 2010;53(7):1554–60.
 42. Passos H, Trindade MP, Vaz TSM, Da Costa LP, Freire MG, Coutinho JAP. The impact of self-aggregation on the extraction of biomolecules in ionic-liquid-based aqueous two-phase systems. *Sep Purif Technol.* 2013;108:174–80.
 43. Freire MG, Cláudio AFM, Araújo JMM, Coutinho JAP, Marrucho IM, Lopes JNC, et al. Aqueous biphasic systems: A boost brought about by using ionic liquids. *Chem Soc Rev.* 2012;41(14):4966–95.
 44. Merchuk J, Andrews B, Asenjo J. Aqueous two-phase systems for protein separation:

- studies on phase inversion. *J Chromatogr B Biom Sci Appl.* 1998;711(285):93.
45. Belchior DCV, Quental M V., Pereira MM, Mendonça CMN, Duarte IF, Freire MG. Performance of tetraalkylammonium-based ionic liquids as constituents of aqueous biphasic systems in the extraction of ovalbumin and lysozyme. *Sep Purif Technol.* 2020;233:116019–29.
 46. Cunha T, Aires-Barros R. Large-scale extraction of proteins. *Appl Biochem Biotechnol - Part B Mol Biotechnol.* 2002;20(1):29–40.
 47. Santos JH, e Silva FA, Ventura SPM, Coutinho JAP, de Souza RL, Soares CMF, et al. Ionic liquid-based aqueous biphasic systems as a versatile tool for the recovery of antioxidant compounds. *Biotechnol Prog.* 2015;31(1):70–7.
 48. Lu M, Tjerneld F. Interaction between tryptophan residues and hydrophobically modified dextran. *J Chromatogr A.* 1997;766:99–108.
 49. Luís A, Dinis TBV, Passos H, Taha M, Freire MG. Good's buffers as novel phase-forming components of ionic-liquid-based aqueous biphasic systems. *Biochem Eng J.* 2015;101:142–9.
 50. Taha M, E Silva FA, Quental M V., Ventura SPM, Freire MG, Coutinho JAP. Good's buffers as a basis for developing self-buffering and biocompatible ionic liquids for biological research. *Green Chem.* 2014;16(6):3149–59.
 51. Pereira MM, Pedro SN, Quental M V., Lima ÁS, Coutinho JAP, Freire MG. Enhanced extraction of bovine serum albumin with aqueous biphasic systems of phosphonium- and ammonium-based ionic liquids. *J Biotechnol.* 2015;206:17–25.
 52. Shahriari S, Tomé LC, Araújo JMM, Rebelo LPN, Coutinho JAP, Marrucho IM, et al. Aqueous biphasic systems: A benign route using cholinium-based ionic liquids. *RSC Adv.* 2013;3(6):1835–43.
 53. Parajó JJ, Macário IPE, Gaetano Y De, Dupont L, Salgado J, Pereira JL, et al. Ecotoxicology and Environmental Safety Glycine-betaine-derived ionic liquids: Synthesis, characterization and ecotoxicological evaluation. *Ecotoxicol Environ Saf.* 2019;184(April):109580.
 54. Pereira MM, Gomes J, Rufino AFCS, Rosa ME, Coutinho AP, Naturelles E, et al. Glycine-Betaine Ionic Liquid Analogues as Novel Phase-Forming Components of Aqueous Biphasic Systems. *Biotechnol Prog.* 2018;34(5):1205–12.
 55. Capela E V., Santiago AE, Rufino AFCS, Tavares APM, Pereira MM, Mohamadou

- A, et al. Sustainable strategies based on glycine-betaine analogue ionic liquids for the recovery of monoclonal antibodies from cell culture supernatants. *Green Chem.* 2019;21(20):5671–82.
56. National Research Council. Integrated Processes. In: *Unit Manufacturing Processes: Issues and Opportunities in Research*. 1995. p. 111–7.
 57. Leite AC, Ferreira AM, Morais ES, Khan I, Freire MG, Coutinho JAP. Cloud Point Extraction of Chlorophylls from Spinach Leaves Using Aqueous Solutions of Nonionic Surfactants. *ACS Sustain Chem Eng.* 2018;6(1):590–9.
 58. Rodrigues MII, Francisco A. Planejamento de Experimentos e Otimização de Processos. C.D.P. Editora, editor. Campinas, Brasil; 2005.
 59. Pereira JFB, Kurnia KA, Cojocarú OA, Gurau G, Rebelo LPN, Rogers RD, et al. Molecular interactions in aqueous biphasic systems composed of polyethylene glycol and crystalline vs. liquid cholinium-based salts. *Phys Chem Chem Phys.* 2014;16(12):5723–31.
 60. Belchior DCV, Almeida MR, Sintra TE, Ventura SPM, Duarte IF, Freire MG. Odd-Even Effect in the Formation and Extraction Performance of Ionic-Liquid-Based Aqueous Biphasic Systems. *Ind Eng Chem Res.* 2019;58(19):8323–31.
 61. Osloob M, Roosta A. Experimental study of choline chloride and K₂HPO₄ aqueous two-phase system, and its application in the partitioning of penicillin G. *J Mol Liq.* 2019;279:171–6.
 62. Reslan M, Kayser V. Ionic liquids as biocompatible stabilizers of proteins. *Biophys Rev.* 2018;10:781–93.
 63. Almeida MR, Belchior DCV, Carvalho PJ, Freire MG. Liquid-Liquid Equilibrium and Extraction Performance of Aqueous Biphasic Systems Composed of Water, Cholinium Carboxylate Ionic Liquids and K₂CO₃. *J Chem Eng Data.* 2019;64(11):4946–55.
 64. Li Z, Liu X, Pei Y, Wang J, He M. Design of environmentally friendly ionic liquid aqueous two-phase systems for the efficient and high activity extraction of proteins. *Green Chem.* 2012;14(10):2941–50.
 65. Du Z, Yu YL, Wang JH. Extraction of proteins from biological fluids by use of an ionic liquid/aqueous two-phase system. *Chem - A Eur J.* 2007;13(7):2130–7.

Appendix A

A 1. Calibration curve for the quantification of the total amount of proteins

Figure A 1 depicts the calibration curve obtained through SE-HPLC and made with BSA.

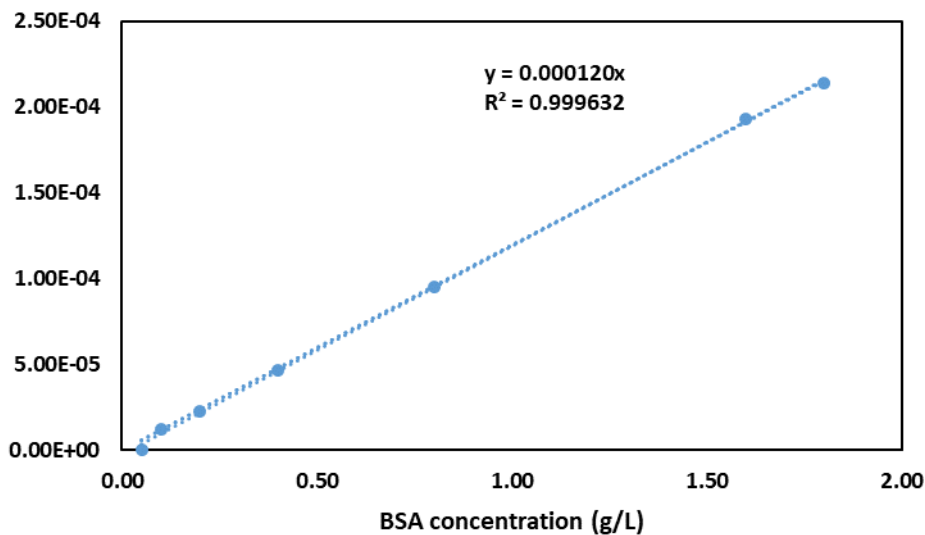


Figure A 1. Calibration curve for total amount of protein.

A 2. Calibration curve for the quantification of the amount of RuBisCO

Figure A 2 depicts the calibration curve obtained through SE-HPLC and made with commercial RuBisCO.

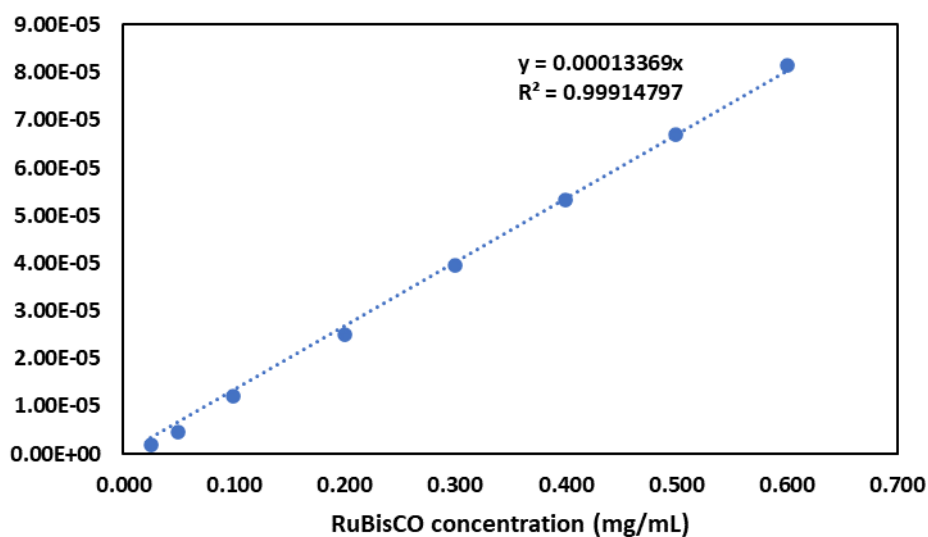


Figure A 2. Calibration curve for RuBisCO quantification.

Appendix B

B 1. Factorial planning for both ILs

Table B 1. exhibits the 2^3 factorial planning for each IL.

Table B 1. 2^3 factorial planning for each IL ([Ch]Cl and [Ch][Acetate]).

Experiment	X ₁	X ₂	X ₃
1	-1	-1	-1
2	1	-1	-1
3	-1	1	-1
4	1	1	-1
5	-1	-1	1
6	1	-1	1
7	-1	1	1
8	1	1	1
9	-1.68	0	0
10	1.68	0	0
11	0	-1.68	0
12	0	1.68	0
13	0	0	-1.68
14	0	0	1.68
15	0	0	0
16	0	0	0
17	0	0	0
18	0	0	0
19	0	0	0
20	0	0	0

B 2. Experimental data and response surface predicted values of the factorial planning for [Ch][Acetate]

Table B 2.1 exhibits the experimental data and response surface predicted values of the factorial planning for RuBisCOs' extraction yield.

Table B 2.1. Experimental data and response surface predicted values of the factorial planning for RuBisCOs' extraction yield.

N°	pH	S/L RATIO	C (M)	Predicted Results	Observed Results	Relative deviation (%)
1	4.50	0.05	0.80	0.280	0.00	
2	9.50	0.05	0.80	7.95	8.79	9.56
3	4.50	0.15	0.80	2.18	0.00	
4	9.50	0.15	0.80	10.8	9.94	-8.73
5	4.50	0.05	2.2	0.400	0.00	
6	9.50	0.05	2.2	8.09	9.00	10.2
7	4.50	0.15	2.2	2.11	0.00	
8	9.50	0.15	2.2	10.8	9.76	-10.1
9	2.80	0.10	1.5	-2.34	0.00	
10	11.2	0.10	1.5	11.4	10.8	-5.10
11	7.00	0.02	1.5	1.75	0.500	-250
12	7.00	0.18	1.5	5.60	8.65	35.3
13	7.00	0.10	0.32	8.06	8.93	9.73
14	7.00	0.10	2.7	8.11	9.04	10.3
15	7.00	0.10	1.5	7.14	7.43	3.96
16	7.00	0.10	1.5	7.14	6.98	-2.28
17	7.00	0.10	1.5	7.14	7.69	7.18
18	7.00	0.10	1.5	7.14	6.29	-13.4
19	7.00	0.10	1.5	7.14	7.22	1.11
20	7.00	0.10	1.5	7.14	6.90	-3.43

Table B 2.2 exhibits the experimental data and response surface predicted values of the factorial planning for RuBisCOs' concentration.

Table B 2.2. Experimental data and response surface predicted values of the factorial planning for RuBisCOs' concentration.

N°	pH	S/L RATIO	C (M)	Predicted Results	Observed Results	Relative deviation (%)
1	4.50	0.05	0.80	0.280	0.00	
2	9.50	0.05	0.80	7.95	8.79	9.56
3	4.50	0.15	0.80	2.18	0.00	
4	9.50	0.15	0.80	10.8	9.94	-8.73
5	4.50	0.05	2.2	0.400	0.00	
6	9.50	0.05	2.2	8.09	9.00	10.2
7	4.50	0.15	2.2	2.11	0.00	
8	9.50	0.15	2.2	10.8	9.76	-10.1
9	2.80	0.10	1.5	-2.34	0.00	
10	11.2	0.10	1.5	11.4	10.8	-5.10
11	7.00	0.02	1.5	1.75	0.500	-250
12	7.00	0.18	1.5	5.60	8.65	35.3
13	7.00	0.10	0.32	8.06	8.93	9.73
14	7.00	0.10	2.7	8.11	9.04	10.3
15	7.00	0.10	1.5	7.14	7.43	3.96
16	7.00	0.10	1.5	7.14	6.98	-2.28
17	7.00	0.10	1.5	7.14	7.69	7.18
18	7.00	0.10	1.5	7.14	6.29	-13.4
19	7.00	0.10	1.5	7.14	7.22	1.11
20	7.00	0.10	1.5	7.14	6.90	-3.43

B 3. Experimental data and response surface predicted values of the factorial planning for [Ch]Cl

Table B 3.1 exhibits the experimental data and response surface predicted values of the factorial planning for RuBisCOs' extraction yield.

Table B 3.1. Experimental data and response surface predicted values of the factorial planning for RuBisCOs' extraction yield.

N°	pH	S/L RATIO	C (M)	Predicted Results	Observed Results	Relative deviation (%)
1	4.50	0.05	0.80	8.73	7.36	-18.7
2	9.50	0.05	0.80	10.2	8.80	-15.5
3	4.50	0.15	0.80	6.36	6.00	-5.96
4	9.50	0.15	0.80	7.41	6.72	-10.3
5	4.50	0.05	2.2	10.4	10.0	-4.29
6	9.50	0.05	2.2	11.9	11.2	-6.82
7	4.50	0.15	2.2	8.56	8.80	2.73
8	9.50	0.15	2.2	9.66	9.92	2.56
9	2.80	0.10	1.5	6.47	7.07	8.52
10	11.2	0.10	1.5	8.61	9.59	10.3
11	7.00	0.02	1.5	12.3	14.1	12.8
12	7.00	0.18	1.5	8.35	8.14	-2.59
13	7.00	0.10	0.32	7.84	9.55	17.9
14	7.00	0.10	2.7	11.2	11.1	-1.13
15	7.00	0.10	1.5	8.45	9.02	6.30
16	7.00	0.10	1.5	8.45	8.72	3.09
17	7.00	0.10	1.5	8.45	7.39	-14.4
18	7.00	0.10	1.5	8.45	7.67	-10.2
19	7.00	0.10	1.5	8.45	8.77	3.64
20	7.00	0.10	1.5	8.45	8.87	4.70

Table B 3.2 exhibits the experimental data and response surface predicted values of the factorial planning for RuBisCOs' concentration.

Table B 3.2. Experimental data and response surface predicted values of the factorial planning for RuBisCOs' concentration.

N°	pH	S/L RATIO	C (M)	Predicted Results	Observed Results	Relative deviation (%)
1	4.50	0.05	0.80	0.516	0.519	0.530
2	9.50	0.05	0.80	0.526	0.581	9.49
3	4.50	0.15	0.80	1.25	1.34	6.74
4	9.50	0.15	0.80	1.37	1.37	-0.036
5	4.50	0.05	2.2	0.410	0.370	-10.9
6	9.50	0.05	2.2	0.541	0.410	-31.9
7	4.50	0.15	2.2	1.12	1.03	-9.36
8	9.50	0.15	2.2	1.37	1.33	-3.29
9	2.80	0.10	1.5	0.703	0.709	0.892
10	11.2	0.10	1.5	0.921	0.973	5.31
11	7.00	0.02	1.5	0.189	0.237	20.2
12	7.00	0.18	1.5	1.50	1.51	0.673
13	7.00	0.10	0.32	1.05	0.940	-11.4
14	7.00	0.10	2.7	0.956	1.12	14.8
15	7.00	0.10	1.5	0.854	0.898	4.90
16	7.00	0.10	1.5	0.854	0.901	5.21
17	7.00	0.10	1.5	0.854	0.744	-14.9
18	7.00	0.10	1.5	0.854	0.777	-9.98
19	7.00	0.10	1.5	0.854	0.905	5.59
20	7.00	0.10	1.5	0.854	0.890	4.04

B 4. Regression coefficients of the predicted second-order polynomial model from RSM using [Ch][Acetate]

Table B 4.1 exhibits the regression coefficients of the predicted second-order polynomial model for the RuBisCOs' extraction yield from RSM.

Table B 4.1. Regression coefficients of the predicted second-order polynomial model for the RuBisCOs' extraction yield from RSM, $R^2 = 0.89709$ and $r_{adj} = 0.80447$.

	Regression Coefficients	Standard deviation	t-student (10)	p-value
Interception	-16.01	7.663	-2.097	0.0624
pH	3.510	1.309	2.682	0.0230
pH²	-0.1482	0.0757	-1.958	0.0787
Solid-liquid Ratio	109.5	59.39	1.844	0.0950
Solid-liquid Ratio²	-489.8	189.2	-2.589	0.0270
IL Concentration	-1.905	4.311	-0.4418	0.6680
IL Concentration²	0.6838	0.9653	0.7083	0.4949
pH x Solid-liquid Ratio	1.918	5.075	0.3779	0.7134
pH x IL Concentration	0.0025	0.3625	0.0069	0.9946
Solid-liquid Ratio x IL Concentration	-1.407	18.13	-0.0776	0.9396

Table B 4.1.1. Effects of the variables in the second-order polynomial model for the extraction yield of RuBisCO.

	Regression Coefficients	Standard deviation	t-student (10)	p-value
Interception	7.137	0.7318	9.752	0.0000
pH	8.158	0.9713	8.399	0.0000
pH²	-1.852	0.9460	-1.958	0.0787
Solid-liquid Ratio	2.287	0.9713	2.354	0.0404
Solid-liquid Ratio²	-2.449	0.9460	-2.589	0.0270
IL Concentration	0.0326	0.9713	0.0336	0.9739
IL Concentration²	0.6701	0.9460	0.7083	0.4949
pH x Solid-liquid Ratio	0.4795	1.269	0.3779	0.7134
pH x IL Concentration	0.0088	1.269	0.0069	0.9946
Solid-liquid Ratio x IL Concentration	-0.0985	1.269	-0.0776	0.9396

Table B 4.2 exhibits the regression coefficients of the predicted second-order polynomial model for the RuBisCOs' concentration from RSM.

Table B 4.2. Regression coefficients of the predicted second-order polynomial model for the RuBisCOs' concentration from RSM, $R^2 = 0.90873$ and $r_{adj.} = 0.82659$.

	Regression Coefficients	Standard deviation	t-student (10)	p-value
Interception	-0.8088	0.9426	-0.8580	0.4110
pH	0.2453	0.1610	1.524	0.1586
pH²	-0.0200	0.0093	-2.144	0.0577
Solid-liquid Ratio	-4.665	7.305	-0.6386	0.5374
Solid-liquid Ratio²	-13.08	23.27	-0.5620	0.5865
IL Concentration	-0.0179	0.5303	-0.0338	0.9737
IL Concentration²	0.0128	0.1187	0.1079	0.9162
pH x Solid-liquid Ratio	2.046	0.6243	3.277	0.0083
pH x IL Concentration	-0.0006	0.0446	-0.0145	0.9887
Solid-liquid Ratio x IL Concentration	-0.0793	2.230	-0.0356	0.9723

Table B 4.2.1. Effects of the variables in the second-order polynomial model for the extraction RuBisCO concentration.

	Regression Coefficients	Standard deviation	t-student (10)	p-value
Interception	0.7488	0.0900	8.318	0.0000
pH	0.8479	0.1195	7.097	0.0000
pH²	-0.2494	0.1164	-2.144	0.0577
Solid-liquid Ratio	0.6922	0.1195	5.794	0.0002
Solid-liquid Ratio²	-0.0654	0.1164	-0.5620	0.5865
IL Concentration	0.0113	0.1195	0.0948	0.9264
IL Concentration²	0.0126	0.1164	0.1079	0.9162
pH x Solid-liquid Ratio	0.5115	0.1561	3.277	0.0083
pH x IL Concentration	-0.0023	0.1561	-0.0145	0.9887
Solid-liquid Ratio x IL Concentration	-0.0056	0.1561	-0.0356	0.9723

B 5. Regression coefficients of the predicted second-order polynomial model from RSM using [Ch]Cl

Table B 5.1 exhibits the regression coefficients of the predicted second-order polynomial model for the RuBisCOs' extraction yield from RSM.

Table B 5.1. Regression coefficients of the predicted second-order polynomial model for the RuBisCOs' extraction yield from RSM, $R^2 = 0.75851$ and $r_{adj.} = 0.54116$.

	Regression Coefficients	Standard deviation	t-student (10)	p-value
Interception	8.737	5.258	1.662	0.1276
pH	1.043	0.8981	1.161	0.2726
pH²	-0.0518	0.0519	-0.9967	0.3424
Solid-liquid Ratio	-75.50	40.75	-1.853	0.0936
Solid-liquid Ratio²	262.2	129.8	2.020	0.0710
IL Concentration	-1.267	2.958	-0.4283	0.6775
IL Concentration²	0.7607	0.6624	1.149	0.2775
pH x Solid-liquid Ratio	-0.7645	3.483	-0.2195	0.8306
pH x IL Concentration	0.0080	0.2487	0.0320	0.9751
Solid-liquid Ratio x IL Concentration	3.471	12.44	0.2791	0.7859

Table B 5.1.1. Effects of the variables in the second-order polynomial model for the extraction yield of RuBisCO.

	Regression Coefficients	Standard deviation	t-student (10)	p-value
Interception	8.453	0.5021	16.83	0.0000
pH	1.269	0.6665	1.903	0.0862
pH²	-0.6470	0.6491	-0.9967	0.3424
Solid-liquid Ratio	-2.320	0.6665	-3.481	0.0059
Solid-liquid Ratio²	1.311	0.6491	2.020	0.0710
IL Concentration	1.985	0.6665	2.978	0.0139
IL Concentration²	0.7455	0.6491	1.148	0.2775
pH x Solid-liquid Ratio	-0.1911	0.8706	-0.2195	0.8306
pH x IL Concentration	0.0279	0.8706	0.0320	0.9751
Solid-liquid Ratio x IL Concentration	0.2430	0.8706	0.2791	0.7859

Table B 5.2 exhibits the regression coefficients of the predicted second-order polynomial model for the RuBisCOs' concentration from RSM.

Table B 5.2. Regression coefficients of the predicted second-order polynomial model for the RuBisCOs' concentration from RSM, $R^2 = 0.95197$ and $r_{adj.} = 0.90875$.

	Regression Coefficients	Standard deviation	t-student (10)	p-value
Interception	0.3896	0.4504	0.8649	0.4074
pH	0.0097	0.0769	0.1261	0.9021
pH²	-0.0024	0.0044	-0.5342	0.6049
Solid-liquid Ratio	6.583	3.491	1.886	0.0886
Solid-liquid Ratio²	-1.257	11.12	-0.1130	0.9122
IL Concentration	-0.4671	0.2534	-1.843	0.0951
IL Concentration²	0.1067	0.0567	1.880	0.0895
pH x Solid-liquid Ratio	0.2366	0.2983	0.7932	0.4461
pH x IL Concentration	0.0172	0.0213	0.8084	0.4377
Solid-liquid Ratio x IL Concentration	-0.1247	1.065	-0.1170	0.9092

Table B 5.2.1. Effects of the variables in the second-order polynomial model for the extraction RuBisCO concentration.

	Regression Coefficients	Standard deviation	t-student (10)	p-value
Interception	0.8540	0.0430	19.85	0.0000
pH	0.1297	0.0571	2.271	0.0465
pH²	-0.0297	0.0556	-0.5342	0.6049
Solid-liquid Ratio	0.7801	0.0571	13.66	0.0000
Solid-liquid Ratio²	-0.0063	0.0556	-0.1130	0.9122
IL Concentration	-0.0545	0.0571	-0.9546	0.3623
IL Concentration²	0.1045	0.0556	1.880	0.0895
pH x Solid-liquid Ratio	0.0592	0.0746	0.7932	0.4461
pH x IL Concentration	0.0603	0.0746	0.8084	0.4377
Solid-liquid Ratio x IL Concentration	-0.0087	0.0746	-0.1170	0.9092

B 6. Pareto charts for the standardized main effects in the factorial planning with [Ch][Acetate]

Figure B 6.1 exhibits the pareto charts for the standardized main effects in the factorial planning for RuBisCOs' extraction yield from RSM.

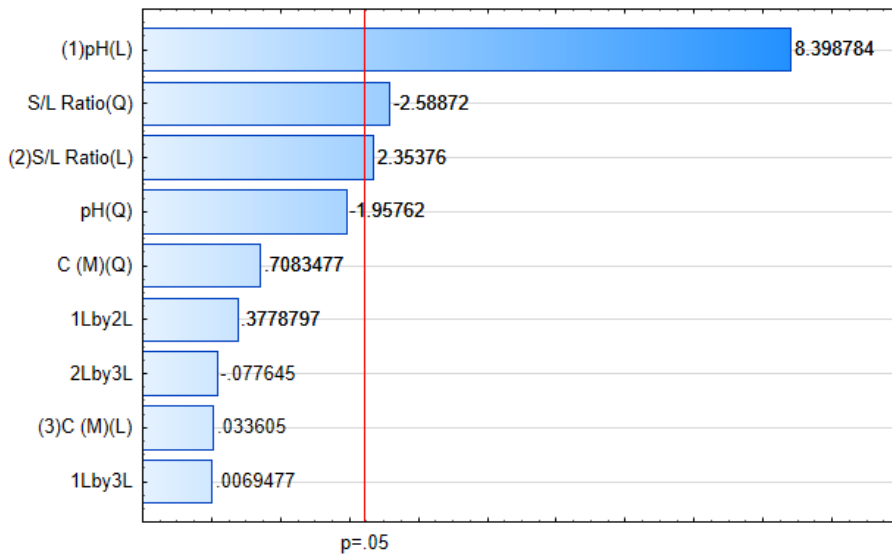


Figure B 6.1. Pareto charts for the standardized main effects in the factorial planning for RuBisCOs' extraction yield. The vertical line indicates the statistical significance of the effects.

Figure B 6.2 exhibits the pareto charts for the standardized main effects in the factorial planning for RuBisCOs' concentration from RSM.

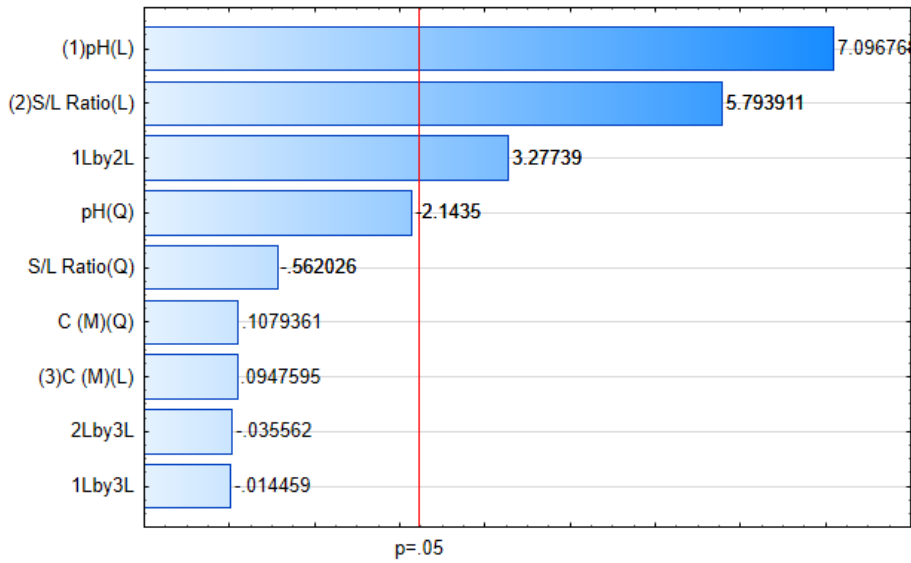


Figure B 6.2. Pareto charts for the standardized main effects in the factorial planning for RuBisCOs' concentration. The vertical line indicates the statistical significance of the effects.

B 7. Pareto charts for the standardized main effects in the factorial planning with [Ch]Cl

Figure B 7.1 exhibits the pareto charts for the standardized main effects in the factorial planning for RuBisCOs' extraction yield from RSM.

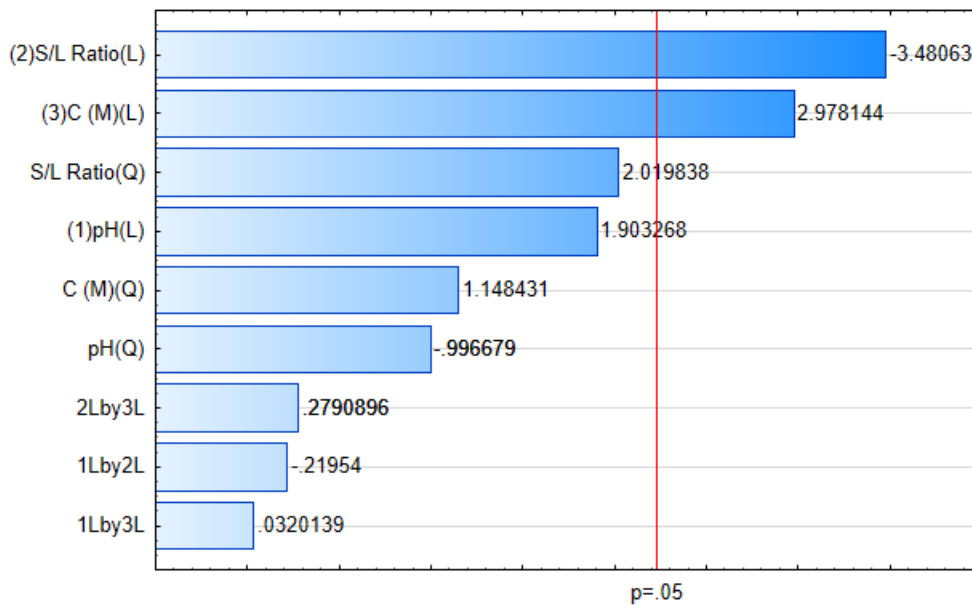


Figure B 7.1. Pareto charts for the standardized main effects in the factorial planning for RuBisCOs' extraction yield. The vertical line indicates the statistical significance of the effects.

Figure B 7.2 exhibits the pareto charts for the standardized main effects in the factorial planning for RuBisCOs' concentration from RSM.

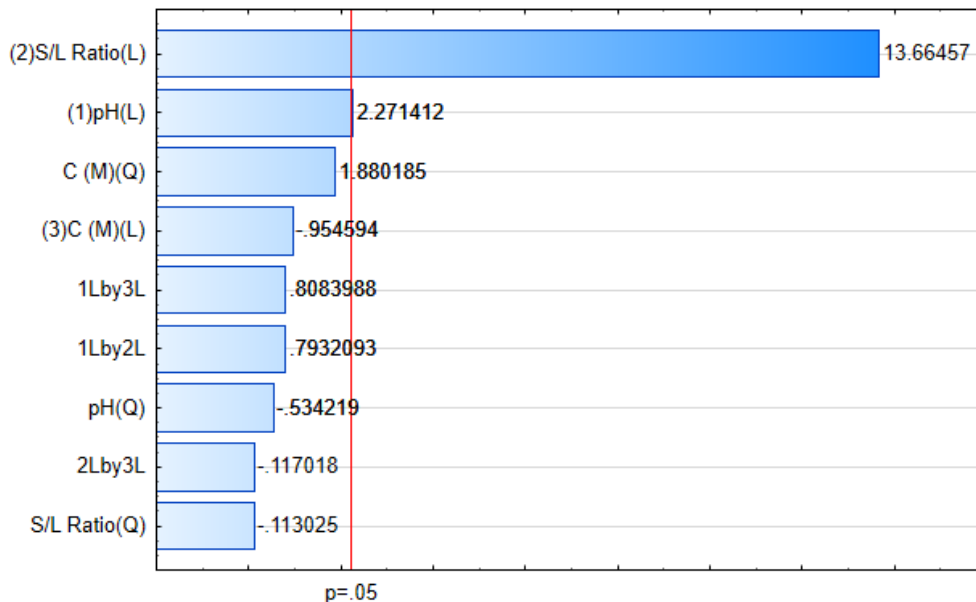


Figure B 7.2. Pareto charts for the standardized main effects in the factorial planning for RuBisCOs' concentration. The vertical line indicates the statistical significance of the effects.

B 8. ANOVA data for the extraction with [Ch][Acetate]

Figure B 8.1 exhibits the ANOVA data for the extraction yield of RuBisCO.

Table B 8.1. ANOVA data for the extraction yield of RuBisCO.

	Sums of squares	Degrees of freedom	Mean square	F-value	p-value
Regression	280.7	9.00	31.19	9.686	0.0007
Residuals	32.20	10.0	3.220		
Total	312.9				

Figure B 8.2 exhibits the ANOVA data for RuBisCO concentration.

Table B 8.2. ANOVA data for RuBisCO concentration.

	Sums of squares	Degrees of freedom	Mean square	F-value	p-value
Regression	4.850	9.00	0.5400	11.06	0.00
Residuals	0.490	10.0	0.0500		
Total	5.340				

B 9. ANOVA data for the extraction with [Ch]Cl

Figure B 9.1 exhibits the ANOVA data for the extraction yield of RuBisCO.

Table B 9.1. ANOVA data for the extraction yield of RuBisCO.

	Sums of squares	Degrees of freedom	Mean square	F-value	p-value
Regression	47.61	9.00	5.291	3.490	0.0322
Residuals	15.16	10.0	1.516		
Total	62.77				

Figure B 9.2 exhibits the ANOVA data for RuBisCO concentration.

Table B 9.2. ANOVA data for RuBisCO concentration.

	Sums of squares	Degrees of freedom	Mean square	F-value	p-value
Regression	2.20	9.00	0.2450	22.02	0.000019
Residuals	0.11	10.0	0.0110		
Total	2.32				

B 10. Profiles for predicted values and desirability in the factorial planning with [Ch][Acetate]

Figure B 10 exhibits the profiles for predicted values and desirability in the factorial planning from RSM.

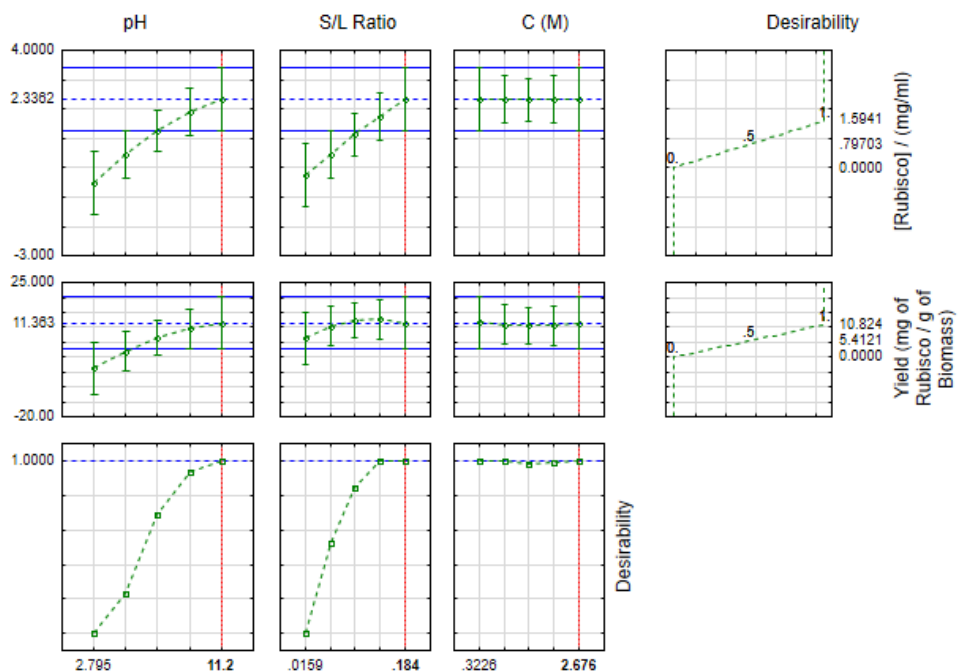


Figure B 10. Profiles for predicted values and desirability in the factorial planning for both dependent variables.

B 11. Profiles for predicted values and desirability in the factorial planning with [Ch]Cl

Figure B 11 exhibits the profiles for predicted values and desirability in the factorial planning from RSM.

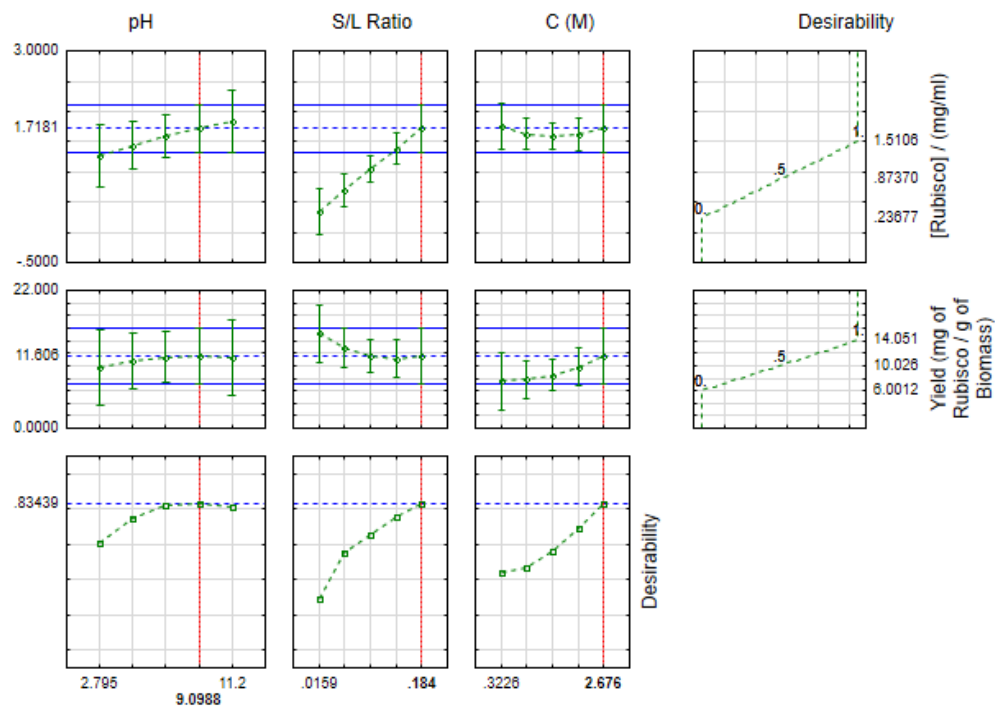


Figure B 11. Profiles for predicted values and desirability in the factorial planning for both dependent variables.

Appendix C

C 1. Experimental binodal data for systems composed of PPG 400 + [Ch][Acetate] + H₂O and PPG 400 + [Ch]Cl + H₂O

The phase diagrams of the ABS used in this work and reported in literature are shown in Figure C 1.

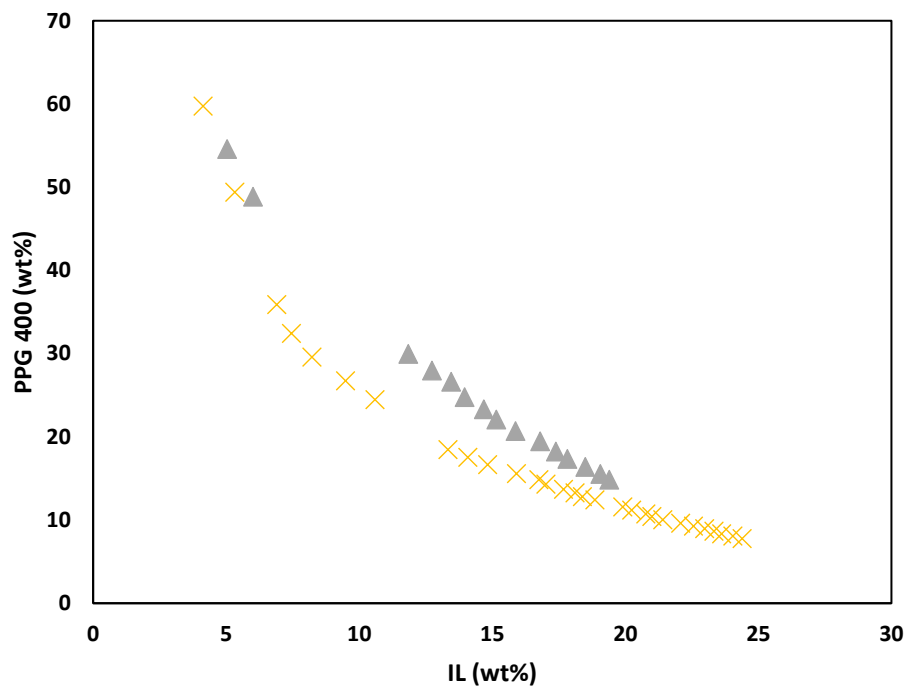


Figure C 1. Phase diagrams for systems composed of PPG 400 + [Ch][Acetate] + H₂O (grey triangles) and PPG 400 + [Ch]Cl + H₂O (yellow crosses) at 25 °C.

The experimental weight fraction data for the phase diagrams of the systems PPG 400 + [Ch][Acetate] + H₂O and PPG 400 + [Ch]Cl + H₂O are presented in Table C 1.

Table C 1. Experimental weight fraction data for the phase diagrams of the systems PPG 400 (1) + [Ch][Acetate] (2) + H₂O (3) and PPG 400 (1) + [Ch]Cl (2) + H₂O (3).

[Ch][Acetate] Mw = 163.2 g/mol		[Ch]Cl Mw = 139.6 g/mol			
100 w ₁	100 w ₂	100 w ₁	100 w ₂	100 w ₁	100 w ₂
54.603	5.039	59.753	4.139	12.819	18.398
48.866	6.010	49.418	5.325	12.429	18.866
29.966	11.852	35.897	6.910	11.610	19.910
27.991	12.734	32.455	7.452	11.194	20.242
26.648	13.465	29.602	8.232	10.746	20.780
24.773	13.970	26.751	9.491	10.434	21.003
23.336	14.687	24.479	10.598	10.068	21.411
22.087	15.158	18.497	13.336	9.617	22.091
20.697	15.883	17.556	14.086	9.301	22.570
19.477	16.800	16.682	14.837	8.985	22.989
18.261	17.389	15.583	15.916	8.657	23.342
17.346	17.830	14.864	16.754	8.352	23.627
16.393	18.499	14.319	17.023	8.084	24.051
15.560	19.067	13.697	17.682	7.773	24.390
14.877	19.400	13.283	18.122		

C 2. Experimental binodal data for systems composed of K₂HPO₄ + [Ch][Acetate] + H₂O and K₂HPO₄ + [Ch]Cl + H₂O

The phase diagrams of the ABS used in this work and reported in literature are shown in Figure C 2.

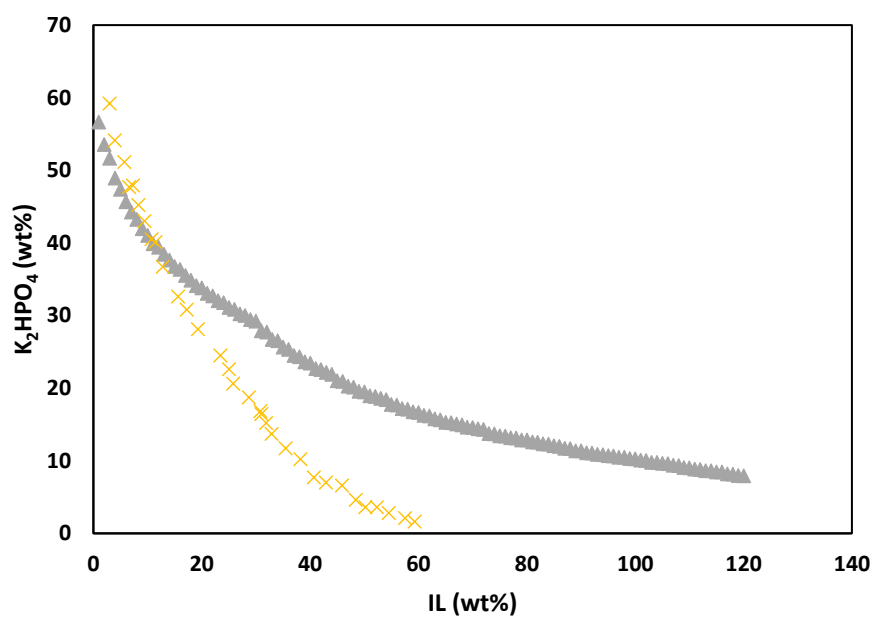


Figure C 2. Phase diagrams for systems composed of $K_2HPO_4 + [Ch][Acetate] + H_2O$ (grey triangles) and $K_2HPO_4 + [Ch]Cl + H_2O$ (yellow crosses) at 25 °C.

The experimental weight fraction data for the phase diagrams of the systems $K_2HPO_4 + [Ch][Acetate] + H_2O$ and $K_2HPO_4 + [Ch]Cl + H_2O$ are presented in Table C 2.

Table C 2. Experimental weight fraction data for the phase diagrams of the systems K_2HPO_4 (1) + [Ch][Acetate] (2) + H_2O (3) and K_2HPO_4 (1) + [Ch]Cl (2) + H_2O (3).

[Ch]Cl Mw = 139.6 g/mol		[Ch][Acetate] Mw = 163.2 g/mol							
100 w_1	100 w_2	100 w_1	100 w_2	100 w_1	100 w_2	100 w_1	100 w_2	100 w_1	100 w_2
59.2	3	56.62	7.79	26.71	23.34	15.21	33.89	10.3	38.98
54.1	3.9	53.55	7.37	26.53	23.18	15.05	34.17	10.27	38.88
51.1	5.7	51.66	9.23	25.64	24.42	14.91	33.87	10.06	39.3
47.9	7.3	48.9	8.74	25.31	24.1	14.61	34.4	10.01	39.1
47.7	6.6	47.35	10.36	24.48	25.27	14.55	34.27	9.78	39.58
45.2	8.3	45.67	9.99	24.32	25.11	14.4	34.53	9.75	39.48
43	9.4	44.23	11.57	23.61	26.13	14.29	34.26	9.62	39.77
40.5	10.7	43.21	11.31	23.45	25.96	13.72	35.28	9.59	39.67
40.1	11.4	41.95	12.73	22.68	27.09	13.67	35.15	9.36	40.16
36.7	12.8	41.02	12.45	22.53	26.91	13.43	35.6	9.31	39.94
32.6	15.6	39.86	13.8	22.15	27.48	13.37	35.46	9.06	40.47
30.8	17.2	39.41	13.64	21.91	27.18	13.17	35.83	9.01	40.26
28.1	19.3	38.4	14.83	21.02	28.5	13.12	35.71	8.83	40.66
24.5	23.4	37.64	14.54	20.9	28.33	12.87	36.16	8.81	40.56
22.6	25	36.74	15.63	20.25	29.31	12.83	36.03	8.64	40.94
20.6	25.8	36.36	15.47	20.14	29.15	12.58	36.5	8.62	40.85
18.7	28.7	35.52	16.51	19.57	30.02	12.53	36.36	8.46	41.19
16.8	30.8	34.85	16.2	19.47	29.86	12.31	36.78	8.42	41
15.2	31.9	34.1	17.14	18.94	30.67	12.26	36.64	8.17	41.56
16.4	31	33.78	16.98	18.85	30.53	12.05	37.06	8.13	41.36
13.7	32.9	33.04	17.91	18.59	30.93	11.97	36.83	7.95	41.79
11.7	35.5	32.71	17.74	18.41	30.62	11.69	37.37	7.91	41.58
10.2	38.2	32.02	18.63	17.75	31.66	11.65	37.24		
7.7	40.7	31.77	18.48	17.65	31.48	11.37	37.79		
7	42.9	31.1	19.36	17.18	32.24	11.33	37.66		
6.6	45.9	30.85	19.2	17.1	32.08	11.09	38.14		
4.6	48.4	30.24	20	16.71	32.71	11.05	38.01		
3.6	50.2	29.98	19.83	16.64	32.57	10.88	38.36		
3.6	52.3	29.43	20.57	16.24	33.22	10.84	38.24		
2.8	54.5	29.2	20.41	16.16	33.06	10.68	38.57		
2.1	57.5	27.89	22.18	15.75	33.75	10.64	38.45		
1.6	59.3	27.69	22.01	15.62	33.47	10.49	38.77		
59.2	3	56.62	7.79	15.28	34.04	10.46	38.66		